8-2015

Strain Promoted Click Chemistry of 2- or 8-Azidopurine and 5-Azidopyrimidine Nucleosides and 8-Azidoadenosine Triphosphate with Cyclooctynes. Application to Living Cell Fluorescent Imaging

Jessica Zayas
Department of Chemistry and Biochemistry, Florida International University

Marie Annoual
Department of Chemistry and Biochemistry, Florida International University, mannoual@fiu.edu

Jayanta K. Das
Department of Environmental & Occupational Health, Florida International University, jdas@fiu.edu

Quentin Felty
Department of Environmental & Occupational Health, Florida International University, feltyq@fiu.edu

Walter Gonzalez
Biomolecular Sciences Institute and Department of Chemistry and Biochemistry, Florida International University, wggonzal@fiu.edu

See next page for additional authors

HHS Public Access

Author manuscript

Bioconjug Chem. Author manuscript; available in PMC 2016 April 10.

Published in final edited form as:

Bioconjug Chem. 2015 August 19; 26(8): 1519–1532. doi:10.1021/acs.bioconjchem.5b00300.

Strain Promoted Click Chemistry of 2- or 8-Azidopurine and 5-Azidopyrimidine Nucleosides and 8-Azidoadenosine Triphosphate with Cyclooctynes. Application to Living Cell Fluorescent Imaging

Jessica Zayas[†], **Marie Annoual**[†], **Jayanta Kumar Das**[‡], **Quentin Felty**[‡], **Walter G. Gonzalez**[†], **Jaroslava Miksovska**[†], **Nima Sharifai**[§], **Akira Chiba**[§], and **Stanislaw F. Wnuk**[†,‡,*]

[†]Department of Chemistry and Biochemistry, Florida International University, Miami, Florida 33199, United States

[‡]Department of Environmental and Occupational Health, Florida International University, Miami, Florida 33199, United States

[§]Department of Biology, University of Miami, Coral Gables, Florida 33146, United States

Abstract

Strain-promoted click chemistry of nucleosides and nucleotides with an azido group directly attached to the purine and pyrimidine rings with various cyclooctynes in aqueous solution at ambient temperature resulted in efficient formation (3 min - 3 h) of fluorescent, *light-up*, triazole products. The 2- and 8-azidoadenine nucleosides reacted with fused cyclopropyl cyclooctyne, dibenzylcyclooctyne or monofluorocyclooctyne to produce click products functionalized with hydroxyl, amino, *N*-hydroxysuccinimide, or biotin moieties. The 5-azidouridine and 5-azido-2′-deoxyuridine were similarly converted to the analogous triazole products in quantitative yields in less than 5 minutes. The 8-azido-ATP quantitatively afforded the triazole product with fused cyclopropyl cyclooctyne in aqueous acetonitrile (3 h). The novel triazole adducts at the 2 or 8 position of adenine or 5-position of uracil rings induce fluorescence properties which were used for direct imaging in MCF-7 cancer cells without the need for traditional fluorogenic reporters. FLIM of the triazole click adducts demonstrated their potential utility for dynamic measuring and tracking of signaling events inside single living cancer cells.

Graphical Abstract

[*]Corresponding Authors: wnuk@fiu.edu, Phone: 305-348-6195.

Author Contributions

The manuscript was written through contributions of all authors. Study concept and design (JZ, SFW), synthesis (JZ, MA), fluorescent microscopy (JKD, QF), photophysical characterization (WG, JM) and FLIM studies (NS, AC). All authors have given approval to the final version of the manuscript.

Notes

The authors declare no competing financial interest.

ASSOCIATED CONTENT

Supporting Information.

Synthetic procedure for the preparation and characterization of **3**, additional fluorescence and cellular imaging data and kinetic data. This material is available free of charge via the Internet at http://pubs.acs.org.

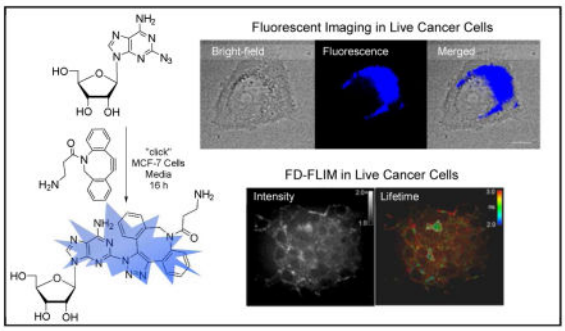

Keywords

Azido nucleosides; Click Chemistry; Cyclooctynes; Pyrimidines; Purines; Fluorescence; Imaging; FLIM

INTRODUCTION

Click chemistry is a common method used for drug discovery, bioconjugation, proteomic profiling and potential identification of cellular targets.[1–3] The strain promoted 1,3-dipolar [3+2] cycloaddition of azides and cyclooctyne (SPAAC) derivatives, first discovered by Bertozzi[4–8] and further developed by Boons,[9] and van Delft,[10–12] occurs readily under physiological conditions in the absence of supplementary reagents such as copper and microwave heating. The SPAAC reactions are also used for the selective modification of compounds or living cells[7,13] including for the imaging of cell surface glycoproteins by fluorescence lifetime imaging microscopy.[14]

Nucleosides, nucleotides and oligonucleotides have now been explored as substrates for click chemistry for some time.[15–17] Bioconjugation of nucleosides and oligonucleotides bearing alkyne modified nucleobases with azide modified fluorescent dyes, sugars and peptides have been well documented.[2,16–19] These coupling reactions usually required Cu(I), a ligand and heating or overnight stirring. Click chemistry of nucleosides and oligodeoxynucleotides (ODNs) with modified sugars bearing terminal alkyne groups have been also explored.[15,17,20–23]

Azide modified sugars,[24–28] such as AZT, have also been studied in click chemistry with typical reaction conditions including the addition of Cu(I) and/or microwave assisted heating. However, the application of the nucleosides bearing an azido group attached directly to the heterocyclic bases in the click chemistry with alkyne partners has received much less attention thus far. This is due to the less developed chemical[28–34] and enzymatic[35–37] synthesis of azido nucleosides and oligonucleotides and their *apparent* lack of compatibility with the solid-phase synthesis of DNA fragments which required trivalent phosphorous-based precursors.[38] Furthermore, Cu^{+}/Cu^{2+} ions often used for click chemistry are known to mediate DNA cleavage.[39]

The 8-azidoadenosine was found to be unreactive with terminal alkyne bearing cyclen Eu^{3+} complexes even after prolonged reaction times (120 h), addition of a large excess of

$CuSO_4 \cdot 5H_2O$, sodium ascorbate and refluxing in DMF.[40] The ribose protected 8-azidoadenosine afforded, however, triazole product in modest yields when treated with (trimethylsilyl)acetylene at 80 °C for 20 h.[41] Similarly, the 2-azidopurine nucleosides were only moderately reactive in copper catalyzed click reactions[42–44] and also required several equivalents of alkyne and prolonged reaction times. These prerequisites are, however, unsuitable for the biological applications including the potential medicinal applications because of the harsh conditions used and cytotoxic effect of the copper catalyst.[45,46] Moreover the coupling between 5-azidouridine and terminal alkynes are also scarcely developed,[47] mainly because of the photochemical instability of the 5-azidouracil substrates.[48] To overcome these limitations the 5-(azido)methyluracil nucleosides were used instead to study the click chemistry of azido-modified pyrimidine bases.[49] Furthermore, the strain promoted click chemistry with cyclooctyne modified phosphate backbone for labeling of DNA[50–52] and RNA,[39,53] has recently been developed.[54]

Naturally occurring nucleic acid components are usually non-fluorescent; therefore, fluorescence has typically been conferred on nucleosides by extending π conjugation of the heterocyclic base[55,56] or by conjugation with known fluorophores.[57,58] Herein, we report a protocol for the convenient strain promoted click chemistry (SPAAC) of 2- or 8-azidoadenine and 5-azidouracil nucleosides and 8-azidoadenosine triphosphate with various cyclooctynes in aqueous solution at ambient temperature and its application to imaging in living cells by *direct* fluorescence light-up.

RESULTS AND DISCUSSION

Synthesis

Reaction between the equivalent amount of 8-azidoadenosine[59] **1** and symmetrically fused cyclopropyl cyclooctyne[10] (OCT) **5** occurred efficiently in an aqueous solution of acetonitrile (ACN) at ambient temperature (3 h) to produce triazole **7** in 96% yield as a mixture[60] of ~1:1 regioisomers after silica gel chromatography or HPLC purification (Scheme 1). This reaction time and efficiency were similar when coupling of **1** and **5** was carried out in MeOH, EtOH or Opti-MEM I cell culture media (see Table S1 in SI section for reaction details). A kinetic analysis of the click reaction between azide **1** and cyclooctyne **5** showed that reaction occurred rapidly (60% conversion in 20 minutes) without the formation of any byproducts (Figure 1). The profile for the reaction was measured by integrating disappearance of the signal of H2 of substrate **1** at 8.07 ppm and appearance of H2 signal at 8.28 ppm for the product **7** on ^{1}H NMR spectra. This reaction displays a second order rate constant of 0.11 $M^{-1}s^{-1}$ which is similar to the previously published data on the reaction of **5** with benzyl azide in the same solvent system (k = 0.14 $M^{-1}s^{-1}$)[10] (see SI section for more details).

The reaction between 8-azido-9-(β-D-arabinofuranosyl)adenine[61] **2** or 8-azido-9-(2-deoxy-2-fluoro-β-D-arabinofuranosyl)adenine **3** (see SI section for the synthesis of **3**) and cyclooctyne **5** also proceeded smoothly (3 h, rt) in ACN/H_2O (3:1) to give triazole **8** or **10**, quantitatively. Analogous treatment of 8-azido-2′-deoxyadenosine[62] **4** with **5** gave the click product **11** (97%). Since biotin tagging is a common *in-vivo* method used for visualization

of proteins and biomolecules with streptavidin, we also demonstrated quantitative labelling of azide **2** with biotin modified OCT **6** to give labeled adduct **9**.

The click reaction of **1** with more complex cyclooctynes including strain modulated dibenzylcyclooctyne[63] (DBCO) **12** or electronic modulated monofluorocyclooctyne[64,65] (MFCO) **16** in polar protic solvents produced the triazoles modified with a terminal amine **13** or "reactive" *N*-hydroxysuccinimide ester **17**, quantitatively as 1:1 mixture of isomers (Scheme 2). The reaction of **1** with **12** required overnight heating at 50 °C, while coupling of **1** and **16** was completed at ambient temperature overnight. Goddard and Bertozzi noted that although the aryl ring fusion may enhance the cyclooctyne ring stain, the sluggish reactivity of DBCO **12** with azides can be attributed to the "flagpole" hydrogen atoms *ortho* to the aryl/cyclooctyne ring junction which decrease reactivity by steric interference with the azide in the transition state.[8,66] Furthermore, azido nucleosides **2** and **4** react with **12** to give the corresponding triazole products **14** and **15**, respectively.

The 2-azidoadenosine **19** also undergoes SPAAC reaction efficiently (Scheme 3). Thus, **19** reacts with cyclooctyne **5** in aqueous media at ambient temperature (3 h) to yield adduct **18** in quantitative yield. Similarly, **19** reacts with **12** to afford triazole **20** but, as noted also above (Scheme 2), the elevated temperature (50 °C) was required for the completion. The natural and 2-substituted purine nucleosides and nucleotides favor an *anti*-glycosyl bond orientation;[67] however, addition of bulky substituents at the C8 position forces a predominantly *syn* conformation in solution because of the unfavorable steric and electrostatic repulsions between the 8-substituent and the ribose ring.[68,69] Thus, the C2 and C8 modified click adducts described here provide analogues with both *syn*- and *anti*-conformations offering the potential for differing cellular targets.

The click reaction between 5-azidouridine[47] **21** and several cyclooctynes including **5**, **6**, **12** or **16** also proceeded efficiently yielding the corresponding novel click adducts **23**, **24**, **25**, **26** and **27**. Thus, treatment of **21** with hydroxyl or biotin modified cyclooctyne **5** or **6** in ACN:H_2O mixture (3:1, *v/v*) afforded **23** or **24** in as fast as 3 minutes at ambient temperature (Scheme 4). Analogous treatment of **21** with free amine modified dibenzylcyclooctyne **12** or NHS modified monofluorocyclooctyne **16** in MeOH gave complete conversion to triazoles **26** or **27** in less than 15 minutes. Furthermore, click reaction of the highly photolyzable 5-azido-2′-deoxyuridine[70] **22** with cyclooctyne **5**, in the ACN/H_2O/MeOH (3:1:1 *v/v/v*) provided corresponding triazole product **25** in excellent yield. The latter coupling must be run in the dark in order to avoid the known photolysis of **22** caused by UV irradiation.[48] Substrate **22** was prepared by conversion of 5-bromo-2′-deoxyuridine[71] to 5-amino derivative followed by Sandmeyer azidation.[70]

Since click chemistry for labeling oligonucleotides are an emerging field,[28,31–33] we established a protocol for SPAAC with azido base modified nucleotides. Thus, reaction of 8-azidoadenosine 5′-triphosphate tetralithium salt **28** and cyclooctyne **5** in aqueous ACN (3 h) quantitatively yielded triazole **29** (Scheme 5). A kinetic analysis of this reaction depicted in Figure 2 shows that reaction occurred efficiently (55% in 35 min, 92% in 2 h) without formation of byproducts. This reaction displays a second order rate constant of 0.07 $M^{-1}s^{-1}$,

which is similar to the previously published data on reaction of **5** with benzyl azide in the same solvent system.[10] (see SI section for more details)

In summary, the efficiency of the SPAAC reaction between azido nucleosides and cyclooctynes strongly depends on the structure of azido and cyclooctyne substrates, whereas the choice of the solvent has less effect. Thus, the 5-azidouracil precursors were significantly more reactive than the 2- or 8-azidoadenine substrates; however, the position of the azido group on the adenine scaffold did not affect reactivity of adenine substrates. As cyclooctynes are concerned, the OCT **5** appeared to be the most reactive towards azido nucleosides followed by MFCO **16** and lastly DBCO **12** (see Table S1 in SI section for a summary of reaction conditions and yields). The selection of solvents for the click reactions was based on substrate solubility. For example, some azido nucleosides (e.g. **1** or **2**) are easily water soluble, while others are not (e.g. **22**) and require methanol to solubilize. Also the hydrocarbon scaffold of the cyclooctynes limits their solubility in aqueous solutions.[72] Typical SPAAC reactions for the uridine substrate **21** with OCT **5**, MFCO **16** or DBCO **12** were completed in 5 min (rt), 12 min (rt) and 15 min (rt), respectively; whereas reactions for the adenosine substrate **1** with the same cyclooctynes required 3 h (rt), 16 h (rt) and 16 h (50 °C), respectively in aqueous ACN or MeOH

Fluorescent Characterization

Unsubstituted nucleosides are typically weakly fluorescent;[73–76] however, substitution at the C2 and C8 position of the purine ring or C5 of the pyrimidine ring with fluorogenic moieties results in nucleosides with fluorescent properties.[19,77,78] While the 8-azido-*arabino*-adenosine **2** has no fluorescence, the click adduct **7** with triazole ring attached *directly* to the imidazolyl ring of purine via a nitrogen atom emits at 300–500 nm with the maximum emission at 376 nm (Φ_{em} = 0.6%, B = 0.13 $M^{-1}cm^{-1}$). Similarly, 5-azidouridine **21** exhibits no noticeable fluorescence, whereas the triazole product **23** shows moderate emission between 285 nm and 550 nm with two emission peaks at 320 nm and 450 nm (Φ_{em} = 1.1%, B = 0.12 $M^{-1}cm^{-1}$). Interestingly, this triazole product showed an excitation maxima at 388 nm which was mainly observed in alkaline phosphate buffer (Figure 3d). A more moderate change in the absorption spectra was observed in MeOH and DMSO (see supplementary data) indicating a ground state deprotonation of the pyrimidine triazole scaffold.

The click adduct **20** of the 2-azidoadenosine **19** and DBCO exhibited the highest fluorescence quantum yield (10.6%), the largest stokes shift (133 nm) and was the brightest (1.74 $M^{-1}cm^{-1}$) of the library of compounds that were prepared and tested. The 2-adenosine-OCT adduct **18** was the second brightest compound (0.38 $M^{-1}cm^{-1}$) and exhibited the second largest extinction coefficient (Table 1).

The effect of solvent polarity was explored for derivatives **7**, **8**, **11**, **13**, **17**, **18**, **20**, **23** and **27** in DMSO and phosphate buffer pH 7.0. We observed a 10 nm and 17 nm bathochromic shift for **11** and **20** upon increasing solvent polarity (from DMSO to phosphate buffer at pH 7.0). Compound **23** showed a more complex spectra upon increase in solvent polarity, with peaks at 324 nm and 440 nm undergoing bathochromic shifts of 10 nm and 5 nm. This uncorrelated shift in emission likely arises from multiple glycosyl bond conformers of **23**

(*syn* vs. *anti*) which are known to exhibit different photophysical properties.[79,80] The amplitude of the fluorescence emission was increased in DMSO for the uracil analogues, when compared to the intensity in MeOH and phosphate buffer. On the other hand, the intensity of the adenine derivatives was enhanced in MeOH and quenched in phosphate buffer, with exception of analogues **7** and **13** which were enhanced in DMSO (Figure S1 in SI section). The observed increase in fluorescence intensity in an aprotic solvent (i.e. DMSO) for the uracil derivatives correlates with the observed ground state deprotonation of the uracil triazole moiety. The solvent effect on **7** and **11** show distinct responses despite their similar scaffolds, indicating that removal of the hydroxyl group at the C2′ likely induces a change in electron delocalization. Furthermore, introduction of a triazole ring at either the C2 or C8 positions likely causes a significant change in conformation (*anti* vs. *syn*) thus changing the solvent sensitivity of the fluorophore, as shown by the OCT adducts **7** and **18** and by the DBCO adducts **13** and **20**.

All triazole products showed a complex fluorescence decay lifetime, with at least a triple discrete model needed to obtain a satisfactory fit (Figure 3), except analogue **8** which showed a biphasic decay. A fast lifetime of 0.1 ns to 0.6 ns was present in all compounds (Table 1). This fast decay is likely due to the fluorescence decay of the heterocyclic bases. In addition, 0.8 ns – 2.3 ns and 4.1 ns – 7.8 ns lifetime was recovered for all compounds, with **26** showing the longest lifetime (7.8 ns). The fractional contribution of each lifetime also varied among all triazole products; however, **11** (19%), **20** (40%) and **23** (38%) showed the largest contribution of the long lifetime (τ_3). The longest average lifetime was observed for **20** (2.8 ns), followed by **23** (2.7 ns), **26** (2.7 ns) and **11** (1.6 ns). The recovered average fluorescence lifetime of the most fluorescent compounds is comparable to the lifetimes of current fluorescent proteins widely used in fluorescence lifetime imaging (FLIM),[81] and the utility of these fluorescent nucleoside analogs as probes in FLIM for real time measuring of metabolic activity inside living cells is discussed below.

Cytotoxicity Assay

Taking advantage that the click reaction between non-fluorescent azido nucleosides and cyclooctynes yields triazole products with strong fluorescence without the necessity for additional modification for visualization, we have tested its application to *in vivo* studies and have demonstrated the viability of these reactions in living cells. A cell toxicity assay was used to determine the non-toxic dose of azides **2** or **21** and cyclooctyne **5** on the survival of MCF-7 cells cultured for a 24 h time period. Under these conditions MCF-7 cells were subjected to the MTT assay that measured the ability of cells to reduce the methylthiazoletetrazolium dye. We measured activity of MCF-7 cells at the most active part of the cells growth phase which was at 50% cell confluency, 24 h after seeding. The *y*-axis of the dose-response graph represents cell viability correlated to metabolic activity. From the dose-response graph for the reaction between cyclooctyne **5** and either azide **2** or **21**, we determined that a 1 μM dosage of these reagents was non-cytotoxic to MCF-7 cells for a 24 h exposure (Figure 4) and, consequently, we utilized this dosage for subsequent fluorescent studies.

Cellular Permeability

A parallel artificial membrane permeation assay (PAMPA)[82] was used to predict cellular permeability of selected azides **2**, **4**, **19** and **23** and triazole adducts **11** and **20**. A correlation between drug permeation across an alkane liquid membrane and percent absorption in humans has previously been shown, thus, a PAMPA assay provides an accurate model in depicting the passive absorption of the tested compounds across a cellular membrane.[83–86] The results showed that approximately 20% of each of the compounds tested passively permeated in through the cellular membrane and into the cells (Table 2). However, since nucleoside transport proteins are also responsible for the cellular uptake of natural and modified nucleosides,[87] one can expect that the membrane proteins might also contribute to the overall uptake of these nucleoside-based theranostics.

In Vivo Images

The click chemistry between 8-azido-*arabino*-Ado **2** and cyclooctyne **5** was carried out in MCF-7 breast cancer cells. Thus, MCF-7 cells were incubated for 3 h at 37 °C with **2** (1 μM). The click reaction commenced via the addition of DMEM/F12 (1:1) 1X cell media containing cyclooctyne **5** (1 μM). We observed strong blue fluorescence in live cells using excitation and absorbance filters 360/40 and 470/40 nm, respectively (Figure 5) which was comparable to the fluorescence that Ito *et al.* observed during the reaction of 8-azido-cAMP and a difluorinated cyclooctyne in HeLa cells.[46] However, contrary to this report, we found that the use of transfection agents (e.g., Lipofectamine, see SI section for discussion), which often results in cytosol fluorescence, undue stress, and morphological changes in cells, was unnecessary.

In our negative controls, background fluorescence was indistinguishable in cells incubated without azide **2** or cyclooctyne **5**. Using a trypan blue fluorescence quenching mechanism,[88] we also concluded that fluorescence was intracellular and not due to the click reaction occurring on the surface of the cell membrane. As shown in Figure 5, the 1 μM dose of compounds **2** and **5** showed a strong fluorescent localization to the nucleus. Similarly, in Figures 6 and 7, the 1 μM dose of azides **19** or **21** and **5** also showed fluorescence localized in the nucleus.

Fluorescence Lifetime Imaging Microscopy

In order to determine fluorescence lifetime within living cells, the frequency-domain fluorescence lifetime imaging microscopy (FD-FLIM) was conducted on MCF-7 cells incubated with the triazole products **8**, **20** or **23**. The FD-FLIM is an imaging technique capable of image acquisition rates that are compatible with *in vivo* imaging, while also offering a means to visualize the individual lifetime components of a sample (i.e. the polar plot histogram).[89] This technique allows one to compare the lifetime characteristics, τ value, of compounds *in vitro* and *in vivo*.

After incubation of MCF-7 cells with triazoles **8**, **20** or **23**, the fluorescent signal from cell nuclei were isolated for lifetime measurement and the average lifetime from multiple cells were calculated for each compound (Table 3, Figure 8). The lifetime value obtained for *arabino* triazole adduct **8** was much higher *in vivo* (2.66 ns) than that found *in vitro* (1.60 ns;

Table 1). This discrepancy in lifetimes suggests that in a methanol solution **8** can exists in two conformations (*syn* and *anti*) which populates the fast lifetime (0.6 ns). We also found that the mean lifetime of triazole **8** was not altered when **8** had been synthesized by an *in vivo* click reaction between azide **2** and cyclooctynes **5** in MCF-7 cells (Table 3, footnote *a*).

The values for click adducts **20** (2.66 ns) and **23** (2.73 ns) were similar to those obtained through spectroscopic methods (see Table 1), although slightly lower. Polar plot analysis reveals that adduct **20** maintains its individual lifetime components (Figure 8), suggesting that the conformation found *in vitro* is also present *in vivo*. We believe that this can be attributed to steric hindrance and the size of the bulky DBCO component. The histogram for adduct **23** indicates that its lifetime components undergo an alteration *in vivo* and in actuality only 1 lifetime population is observed. As shown in Figure 3d and in the SI data, this compound is the most sensitive of all the compounds tested to pH and solvent polarity thus it is not entirely surprising to see differences between fluorescence lifetimes *in vitro* and within living cells. In addition to featuring a different solvent, the intranuclear environment may introduce a higher pH[90] or π-orbital stacking when compounds are DNA-bound, both of which can alter the fluorescence lifetime characteristics of a given compound.[91,92]

Although the lifetime properties of **8** and **23** change slightly within cells compared to *in vitro* determination, we found that their intracellular lifetimes are also relatively consistent from cell to cell and thus prove unambiguously the presence of **8**, **20** and **23** within the nucleus. Therefore, all three compounds can serve as viable fluorescent probes *in vivo*, with adduct **20** being the compound of choice when low environmental sensitivity (i.e. lifetime invariance) is desired.

The present *in situ* click chemistry drug delivery system represents a novel approach wherein both a therapeutic effect and drug uptake-related imaging information may be produced and readily monitored at the cellular level. Although it's beyond the scope of this paper, the long-term implications of this *in situ* click chemistry drug delivery strategy embodied in click substrates (e.g., **2**, **19** and **21)** could allow for a more precise monitoring of dosage levels, as well as an improved understanding of cellular uptake. It is also noteworthy that our nucleobase-derived triazole adducts can be visualized using fluorescent microscopy and FLIM without reliance on auxiliary fluorescent reporters such as green-fluorescent proteins[93] or Alexa Fluor.[14]

CONCLUSIONS

We have developed an efficient strain-promoted click chemistry between 2- or 8-azidoadenine and 5-azidouracil nucleosides as well as 8-azidoadenosine triphosphate with various cyclooctynes to produce highly functionalized triazole products. The reactions occur in cell culture media or aqueous organic solution at ambient temperature without the assistance of copper and/or microwave heating. We discovered that 5-azidouridine substrates were significantly more reactive than the 2- or 8-azidoadenosine precursors, whereas the position of the azido group on the adenine scaffold did not affect reactivity of adenosine substrates. We found that the novel triazole products have sufficient fluorescent properties which were used for direct imaging in living MCF-7 cancer cells without the need of any

extra fluorophores. Using fluorescence lifetime imaging (FLIM) of living cancer cells, we have demonstrated, for the first time, the potential utility of triazole modified nucleobases for dynamic measuring and tracking of signaling events inside single living cells.

EXPERIMENTAL PROCEDURES

Materials and General Methods—Detailed methods and characterization can be found in the Supporting Information. The ^{1}H (400 MHz), ^{19}F NMR (376.4 MHz) and ^{13}C (100.6 MHz) were recorded at ambient temperature in solutions of ACN-d_3, D_2O, or DMSO-d_6, as noted. The reactions were followed by TLC with Merck Kieselgel 60-F254 sheets, and products were detected with a 254 nm light. Column chromatography was performed using Merck Kieselgel 60 (230–400 mesh). Reagent-grade chemicals were used. Azido nucleoside substrates were prepared as described in literature (**1**,[59] **2**,[61] **4**,[62] and **22**[70]) or in SI section (**3**), or are commercially available (**19**, **21** and **28)** from Carbosynth. Cyclooctynes **5**, **6**, **12** and **16** are commercially available from Kerafast, SynAffix, Sigma Aldrich or Berry & Associates. Lipofectamine LTX and Plus reagent was purchased from Invitrogen. HPLC analysis was performed on a semi-preparative Phenomenex Gemini RP-C18 column (5 μ, 25 cm × 1 cm) with UV detection at 254 nm.

Synthetic Procedures

8-(1,2,3-Triazol-1*H*-yl)adenosine-OCT adduct (7). Typical Procedure— Cyclooctyne **5** (*endo*; 7.6 mg, 0.05 mmol) was added to a stirred solution of 8-azidoadenosine[59] **1** (15.0 mg, 0.05 mmol) in a mixture of ACN/H_2O (3:1, 1 mL) at ambient temperature. After 3 h, the volatiles were evaporated *in vacuo* and the resulting residue was purified on silica gel column chromatography (20% MeOH/EtOAc) to give **7** as mixture of regioisomers (1:1; 21.0 mg, 96%) as a white solid. Alternatively the crude reaction mixture was passed through a 0.2 μm PTFE syringe filter, and then purified on the semipreparative HPLC column (17% ACN/H_2O, 2.0 mL/min) to give **7** (1:1; 21.0 mg, 96%) as a white solid (t_R = 4.5–8.2 min): UV λ_{max} 270 nm (ε 21 100), λ_{min} 241 nm (ε 12 100); ^{1}H NMR (DMSO-d_6) δ 0.84–0.95 (m, 2H, Hγ), 0.99 (“q”, J = 9.4 Hz, 0.5H, CH cyclopropyl), 1.00 (q, J = 9.4 Hz, 0.5H, CH cyclopropyl), 1.51–1.74 (m, 2H, Hβ), 2.00–2.19 (m, 2H, Hβ), 2.57–2.67 (m, 1H, Hα), 2.77–2.87 (m, 1H, Hα), 2.87–2.99 (m, 1H, Hα), 3.09– 3.15 (m, 1H, Hα), 3.42–3.53 (m, 3H, CH_2 & H5′), 3.58 (“dq” J = 12.2, 4.2 Hz, 1H, H5″), 3.85–3.93 (m, 1H, H4′), 4.00–4.07 (m, 1H, H3′), 4.35 (t, J = 4.9 Hz, 1H, OH), 4.93 (“q”, J = 5.2 Hz, 0.5H, H2′), 5.00 (“q”, J = 5.2 Hz, 0.5H, H2′), 5.12–5.23 (m, 2H, H1′ & OH), 5.36–5.52 (m, 2H, 2 x OH), 7.78 (br s, 2H, NH_2), 8.23 (s, 1H, H2); ^{13}C NMR (CD_3CN) δ 18.44, 18.58, 18.62, 20.14, 20.22, 20.82, 20.88, 21.21, 21.30, 22.33, 22.44, 25.04, 58.02, 58.81, 62.08, 69.18, 70.83, 71.01, 72.39, 72.44, 72.56, 86.96, 87.05, 89.39, 90.92, 138.39, 138.42, 138.47, 144.87, 144.93, 148.52, 152.01, 153.35, 156.31; HRMS (ESI^+) *m/z* calcd $C_{20}H_{27}N_9O_5$ $(M+H)^+$: 459.2054, found: 459.2050

Note: Analogous treatment of **1** (7.0 mg, 0.023 mmol) with **5** (4.7:1, *exo-endo*; 3.4 mg, 0.023 mmol) also gave **7** (~1:1; 10.0 mg, 96%).

9-(β-D-Arabinofuranosyl)-8-(1,2,3-triazol-1*H*-yl)adenine-OCT adduct (8)— Cyclooctyne **5** (4.7:1, *exo-endo*; 4.9 mg, 0.02 mmol) was added to a stirred solution of **2**[61] (10.0 mg, 0.02 mmol) in a mixture of ACN/H_2O (3:1, 1 mL) at ambient temperature. After 1 h, the volatiles were evaporated *in vacuo* and the resulting residue was purified by column chromatography on silica gel (EtOAc → 20% MeOH/EtOAc) to give **8** as mixture of regioisomers (~1:1; 12.8 mg, 93%) as a white solid: UV λ_{max} 273 nm (ε 17 500), λ_{min} 248 nm (ε 8700); ^{1}H NMR (DMSO-d_6) δ 0.83–0.96 (m, 2H, 2 x Hγ), 0.96–1.07 (m, 1H, CH cyclopropyl), 1.50–1.70 (m, 2H, 2 x Hβ), 2.01–2.19 (m, 2H, 2 x Hβ), 2.56–2.71 (m, 1H, Hα), 2.78–2.95 (m, 2H, 2 x Hα), 3.11 (“q”, *J* = 3.3 Hz, 0.5H, Hα), 3.15 (“q”, *J* = 3.6 Hz, 0.5H, Hα), 3.46–3.53 (m, 1H, H5′), 3.58–3.66 (m, 3H, H5″ & *CH*$_2$OH), 4.20 (q, 1H, *J* = 5.6 Hz, H4′), 4.26–4.37 (m, 1H, H2′ & H3′), 5.08–5.15 (m, 1H, OH), 5.41 (br s, 1H, OH), 5.63–5.67 (m, 1H, OH), 5.69 (d, *J* = 6.7 Hz, 0.5H, H1′), 5.71 (d, *J* = 6.8 Hz, 0.5, H1′), 7.61 (s, 2H, NH_2), 8.23 (s, 1H, H2); ^{13}C NMR (DMSO-d_6) δ 13.34, 17.42, 17.49, 19.31, 19.84, 19.87, 20.36, 20.38, 21.65, 24.12, 24.17, 30.09, 35.23, 56.57, 59.73, 73.17, 73.28, 75.17, 75.24, 81.61, 81.69, 84.24, 84.27, 115.79, 137.15, 137.18, 137.42, 137.43, 143.29, 143.34, 148.43, 152.46, 154.95, 162.35; HRMS (ESI$^+$) *m/z* calcd $C_{20}H_{26}N_8NaO_5$ $(M+Na)^+$: 481.1918, found: 481.1927.

9-(β-D-Arabinofuranosyl)-8-(1,2,3-triazol-1*H*-yl)adenine-OCT-biotin adduct (9)— Cyclooctyne **6** (*endo*; 5.5 mg, 0.01 mmol) was added to a stirred solution of **2** (3.1 mg, 0.01 mmol) in a mixture of ACN/H_2O (3:1, 1 mL) at ambient temperature. After 2 h (TLC showed complete conversion to the more polar product), the volatiles were evaporated *in vacuo* and the resulting residue was purified by HPLC (as described for **7**) to give **9** (5.4 mg, 71%) as a white oil: HRMS (ESI$^+$) *m/z* calcd $C_{20}H_{26}N_8NaO_5$ $(M+Na)^+$: 481.1918, found: 481.1927.

9-(2-Deoxy-2-fluoro-β-D-arabinofuranosyl)-8-(1,2,3-triazol-1*H*-yl)adenine-OCT adduct (10)— Cyclooctyne **5** (*exo:endo,* 4.7:1; 3.7 mg, 0.025 mmol) was added to a stirred solution of **3** (7.6 mg, 0.025 mmol) in a mixture of ACN/H_2O (3:1, 1 mL) at ambient temperature. After 3 h (TLC and NMR showed complete conversion of **3** to **10**) the volatiles were evaporated *in vacuo* to give **10** as mixture of regioisomers (~1:1; 11 mg, 98%) as a white solid: ^{1}H NMR (DMSO-d_6) δ 0.84–0.97 (m, 2H, 2 x Hγ), 0.98–1.07 (m, 1H, CH cyclopropyl), 1.52–1.71 (m, 2H, 2 x Hβ), 2.00–2.19 (m, 2H, 2 x Hβ), 2.56–2.72 (m, 1H, Hα), 2.73–2.95 (m, 2H, 2 x Hα), 3.09–3.16 (m, 1H, Hα), 3.46–3.53 (m, 2H, *CH*$_2$OH), 3.54–3.67 (m, 2H, H5′ & H5″), 3.69–3.75 (m, 1H, OH), 4.31–4.38 (m, 1H, OH), 4.63–4.77 (m, 1H, H4′), 5.06–5.12 (m, 1H, H3′), 5.23 (dt, *J* = 53.9, 5.7 Hz, H2′), 5.86–5.95 (m, 2H, H1′ & OH), 7.00 (br s, 2H, NH_2), 8.27 (s, 0.5H, H2), 8.28 (s, 0.5H, H2); ^{19}F NMR (DMSO-d_6) δ −198.52 (ddd, *J* = 53.9, 21.4, 8.2 Hz, 0.5F), −199.01 (ddd, *J* = 53.9, 21.5, 7.3 Hz, 0.5F); HRMS (ESI$^+$) *m/z* calcd $C_{20}H_{26}FN_8O_4$ $(M+H)^+$: 461.2056, found: 461.2059.

2′-Deoxy-8-(1,2,3-triazol-1*H*-yl)adenosine-OCT adduct (11)— Cyclooctyne **5** (*endo*; 15.7 mg, 0.1 mmol) was added to a stirred solution of **4**[62] (29.5 mg, 0.1 mmol) in a mixture of ACN/H_2O (3:1, 1 mL) at ambient temperature. After 3 h, the crude reaction mixture was passed through a 0.2 μm PTFE syringe filter, and then purified on the semipreparative HPLC column (17% ACN/H_2O, 2.0 mL/min) to give **11** as mixture of regioisomers (1:1; 49.3 mg,

96%) as a white solid (t_R = 13.0–16.2 min): UV λ_{max} 272 nm (ε 18 200), λ_{min} 238 nm (ε 8500); ^{1}H NMR (DMSO-d_6) 0.82–0.95 (m, 2H, 2 x Hγ), 0.96–1.07 (m, 1H, CH cyclopropyl), 1.53–1.72 (m, 2H, 2 x Hβ), 2.03–2.19 (m, 3H, H2′ & 2 x Hβ′), 2.60–2.72 (m, 2H, 2 x Hα), 2.81–2.97 (m, 2H, 2 x Hα), 3.03–3.18 (m, 3H, H2″ & 2 x Hα), 3.37–3.45 (m, 1H, H5′), 3.47–3.59 (m, 3H, H5′ & *CH$_2$OH*), 3.76–3.82 (m, 1H, H4′), 4.30–4.37 (m, 2H, H3′ & OH), 5.26 (d, *J* = 4.0 Hz, 1H, OH), 5.27–5.34 (m, 1H, OH), 5.71 (dd, *J* = 6.4, 3.1 Hz, 0.5H, H1′), 5.73 (dd, *J* = 6.4, 3.2 Hz, 0.5H, H1′), 7.72 (br s, 2H, NH_2), 8.26 (s, 1H, H2); HRMS (ESI$^+$) *m/z* calcd $C_{20}H_{27}N_8O_4$ $(M+H)^+$: 443.2150, found: 443.2142.

8-(1,2,3-Triazol-1*H*-yl)adenosine-DBCO adduct (13)—Cyclooctyne **12** (15.0 mg, 0.055 mmol) was added to a stirred solution of **1** (16.4 mg, 0.055 mmol) in a mixture of ACN/H_2O (3:1, 1.5 mL) at 50 °C. After 16 h, the crude reaction mixture was passed through a 0.2 μm PTFE syringe filter, and then injected into a semipreparative HPLC column (40% ACN/H_2O 1.0 mL/min) to give **13** (10.6 mg, 98%) as a mixture of several inseparable regioisomers (t_R = 15.5–23.0 min): UV λ_{max} 276 nm (ε 16 000), λ_{sh} 307 nm (ε 11 200), λ_{min} 270 nm (ε 14 500). Two major isomers (~85–90% of total isomeric composition) had: ^{1}H NMR (DMSO-d_6) δ 1.64–1.78 (m, 2H, NH_2), 2.08–2.33 (m, 2H, C*H$_2$*CO), 2.67–2.81 (m, 2H, C*H$_2$*NH_2), 3.31–4.18 (m, 4H, H3′, H4′, H5′ & H5″), 4.59 (“dm”, *J* = 17.1 Hz, 1H, CH_2), 5.08–5.18 (m, 1H, H2′), 5.19–5.55 (m, 3H, 3 x OH), 5.72 (d, *J* = 7.5 Hz, 0.5H, H1′), 5.83 (d, *J* = 7.0 Hz, 0.5H, H1′), 5.96 (br d, *J* = 17.6 Hz, 1H, CH_2), 6.09 (br d, *J* = 17.4 Hz, 1H, CH_2), 7.26–7.56 (m, 8H, H_{ar}), 8.25 (s, 0.5H, H2), 8.28 (s, 0.5H, H2); HRMS (ESI$^+$) *m/z* calcd $C_{28}H_{29}N_{10}O_5$ $(M+H)^+$: 585.2317, found: 585.2330.

9-(β-D-Arabinofuranosyl)-8-(1,2,3-triazol-1*H*-yl)adenine-DBCO adduct (14)—Cyclooctyne **12** (5.72 mg, 0.02 mmol) was added to a stirred solution of **2** (4.0 mg, 0.02 mmol) in MeOH (1 mL) at 50 °C. After 16 h, the crude reaction mixture was passed through a 0.2 μm PTFE syringe filter, and then injected into a semipreparative HPLC column (Phenomenex Gemini RP-C18 column; 5 μ, 25 cm × 1 cm) (40% ACN/H_2O, 1.5 mL/min) to give **14** (8.52 mg, 95%) as a mixture of several inseparable regioisomers (t_R = 5.5–10.0 min): ^{1}H NMR (DMSO-d_6) δ Two major isomers (~85–90% of total isomeric composition) had: ^{1}H NMR (DMSO-d_6) δ 1.42–1.78 (m, 2H, NH_2), 2.01–2.17 (m, 2H, C*H$_2$*CO), 2.60–2.78 (m, 2H, C*H$_2$*NH_2), 3.17–3.24 (m, 2H, H4′ & H5′), 3.28 (dd, *J* = 11.5 Hz, 4.6 Hz, 1H, H5″), 3.83–3.87 (m, 1H, H3′), 4.10 (t, *J* = 6.0 Hz, 0.5H, H2′), 4.11 (t, *J* = 5.9 Hz, 0.5H, H2′), 4.49 (br s, 2H, CH_2), 5.72 (d, *J* = 5.1 Hz, 1H, H1′), 7.26–7.56 (m, 8H, H_{ar}), 8.09 (s, 1H, H2); HRMS (ESI$^+$) *m/z* calcd $C_{28}H_{29}N_{10}O_5$ $(M+H)^+$: 585.2317, found: 585.2425.

2′-Deoxy-8-(1,2,3-triazol-1*H*-yl)adenosine-DBCO adduct (15)—Cyclooctyne **12** (4.7 mg, 0.015 mmol) was added to a stirred solution of **4** (4.9 mg, 0.015 mmol) in MeOH (1.5 mL) at 50 °C. After 16 h, the crude reaction mixture was passed through a 0.2 μm PTFE syringe filter, and then injected into a semipreparative HPLC column (Phenomenex Gemini RP-C18 column; 5 μ, 25 cm × 1 cm (40% ACN/H_2O, 2.0 mL/min) to give **15** (9.5 mg, 95%) as a mixture of several inseparable regioisomers (t_R = 8.5–5.0 min): UV λ_{max} 273 nm (ε 12 550); ^{1}H NMR (DMSO-d_6) δ 1.64–1.81 (m, 2H, NH_2), 2.11–2.15 (m, 1H, H2′), 2.15–2.30 (m, 2H, CH_2CO), 2.60–2.79 (m, 2H, C*H$_2$*NH_2), 3.34–3.95 (m, 4H, H3′, H4′, H5′ & H5″), 4.51–4.60 (m, 2H, CH_2), 4.91 (dd, *J* = 5.8, 2.3 Hz, 1H, H2′), 5.18–5.48 (m, 3H, 3 x OH),

5.74 (d, *J* = 6.7 Hz, 0.5H, H1′), 5.76 (d, *J* = 6.2 Hz, 0.5H, H1′), 5.94 (br d, *J* = 15.8 Hz, 1H, CH_2), 6.12 (br d, *J* = 16.4 Hz, 1H, CH_2), (6.86–7.84 (m, 8H, H_{ar}), 8.4 (s, 0.5H, H2), 7.94 (s, 0.5H, H2); HRMS (ESI^+) m/z calcd $C_{28}H_{29}N_{10}O_4$ $(M+H)^+$: 569.2368, found: 569.2411.

8-(1,2,3-Triazol-1*H*-yl)adenosine-MFCO adduct (17)—Cyclooctyne **16** (6.25 mg, 0.02 mmol) was added to a stirred solution of **1** (6.25 mg, 0.02 mmol) in MeOH (1 mL) at ambient temperature. After 16 h, the volatiles were evaporated *in vacuo* to give cycloadduct **17** (1:1; 12.3 mg, 98%) as a clear oil: UV λ_{max} 271 nm (ε 16 400), λ_{min} 242 nm (ε 8000); ^1H NMR (DMSO-d_6/D_2O) δ 1.43–1.50 (m, 6H, 3 x CH_2), 1.56–1.67 (m, 4H, 2 x CH_2), 1.67–1.75 (m, 2H, CH_2), 2.23–2.34 (m, 2H, CH_2), 2.54–2.60 (m, 2H, CH_2), 2.60–2.67 (m, 2H, CH_2), 2.76–2.82 (br s, 4H, 2 x CH_2), 3.04–3.13 (m, 2H, CH_2), 3.45 (“dd”, *J* =, 10.8, 2.3 Hz, 1H, H5′), 3.51 (“dd”, *J* = 2.2 Hz, 10.9 Hz, 1H, H5″), 3.87–3.90 (m, 0.5H, H4′), 3.91–3.95 (m, 0.5H, H4′), 4.03 (m, 0.5H, H3′), 4.09 (m, 0.5H, H3′), 4.97 (t, *J* = 4.9 Hz, 0.5H, H2′), 4.98 (t, *J* = 5.1 Hz, 0.5H, H2′), 5.27 (d, *J* = 7.0 Hz, 0.5 H, H1′), 5.28 (d, *J* = 7.1 Hz, 0.5 H, H1′), 8.27 (s, 0.5H, H2), 8.28 (s, 0.5H, H2); HRMS (ESI^+) *m/z* calcd $C_{29}H_{37}FN_{10}NaO_9$ $(M+Na)^+$: 711.2621, found: 711.2543.

2-(1,2,3-Triazol-1*H*-yl)adenosine-OCT adduct (18)—Cyclooctyne **5** (4.7:1 *exo-endo* mixture; 3.13 mg, 0.020 mmol) was added to a stirred solution of 2-azidoadenosine[94] **19** (6.25 mg, 0.020 mmol) in a mixture of ACN/H_2O (3:1, 1 mL) at ambient temperature. After 2 h, the volatiles were evaporated *in vacuo* to give **18** (9.3 mg, 100%) as a white solid: UV λ_{max} 261 nm (ε 19 100), λ_{min} 246 nm (ε 16 600); ^1H NMR (DMSO-d_6) δ 0.81–0.89 (m, 2H, 2 x Hγ), 0.94–1.04 (m, 1H, CH cyclopropyl), 1.56–1.72 (m, 2H, 2 x Hβ), 2.06–2.22 (m, 2 H, 2 x Hβ), 2.81–2.90 (m, 1H, Hα), 2.99–3.14 (m, 2H, 2 x Hα), 3.15–3.19 (m, 1H, Hα), 3.44–3.58 (m, 3H, H5′ & CH_2), 3.59–3.69 (m, 1H, H5′), 4.11–4.16 (m, 1H, H4′), 4.35 (t, *J* = 5.0 Hz, 1H, H3′), 4.59 (“quint”, *J* = 6.0 Hz, 1H, H2′), 4.99–5.04 (m, 1H, OH), 5.21 (d, *J* = 4.9 Hz, 1H, OH), 5.45–5.53 (m, 2H, 2 x OH), 5.89 (d, *J* = 5.8 Hz, 1H, H1′), 7.89 (br s, 2H, NH_2), 8.52 (s, 1H, H8); HRMS (ESI^+) *m/z* calcd $C_{20}H_{27}N_9O_5$ $(M+H)^+$: 459.2099, found: 459.2098.

2-(1,2,3-Triazol-1*H*-yl)adenosine-DBCO adduct (20)—Cyclooctyne **12** (9.67 mg, 0.035 mmol) was added to a stirred solution of **19** (10.93 mg, 0.035 mmol) in MeOH (1 mL) at ambient temperature. After 16 h, the volatiles were evaporated *in vacuo* and the residue was passed through a 0.2 μm PTFE syringe filter, and then purified on the semipreparative HPLC column (17% ACN/H_2O, 2.0 mL/min) to give **20** (17.5 mg, 85%) as a mixture of several inseparable isomers (t_R = 13.0–16.2 min): UV λ_{max} 263 nm (ε 16 400), λ_{sh} 274 nm (ε 9 600), λ_{min} 253 nm (ε 15 200); Two major isomers (~85–90% of total isomeric composition) had: ^1H NMR (DMSO-d_6) δ 1.58–1.62 (m, 2H, NH_2), 2.03–2.09 (m, 2H, C*H*$_2$CO), 2.57–2.72 (m, 2H, C*H*$_2$$NH_2$), 3.49–3.50 (m, 1H, H5′), 3.69 (dd, *J* = 11.8 Hz & 3.3 Hz, 1H, H5″), 3.83–3.94 (m, 1H, H4′), 4.07–4.16 (m, 1H, H3′), 4.38 (t, *J* = 5.1 Hz, 0.5H, H2′), 4.44 (t, *J* = 5.0 Hz, 0.5H, H2′), 4.53 (“dm”, *J* = 17.0 Hz, 1H, CH_2), 4.86–5.47 (m, 3H, 3 x OH), 5.67 (d, *J* = 7.1 Hz, 0.5H, H1′), 5.82 (d, *J* = 7.2 Hz, 0.5H, H1′), 5.96 (br d, *J* = 19.7 Hz, 2H, CH_2), 7.06–7.52 (m, 8H, H_{ar}), 8.54 (s, 0.5H, H8), 8.55 (s, 0.5H, H8); HRMS (ESI^+) *m/z* calcd $C_{28}H_{29}N_{10}O_5$ $(M+H)^+$: 585.2317, found: 585.2318.

5-(1,2,3-Triazol-1*H*-yl)uridine-OCT adduct (23)—Cyclooctyne **5** (4.0 mg, 0.025 mmol) was added to a stirred solution of 5-azidouridine **21** (7.3 mg, 0.025 mmol) in a mixture of ACN/H_2O (3:1, 1 mL) at ambient temperature. After 15 min, the volatiles were evaporated *in vacuo*, and the oily residue was passed through a 0.2 μm PTFE syringe filter, and then purified on the semipreparative HPLC column (20% ACN/H_2O, 2.0 mL/min; t_R = 5.2 – 8.0 min) to give **23** (6.2 mg, 77%) as a 1:1 mixture of isomers: UV λ_{max} 270 nm (ε 10 100) λ_{min} 248 nm (ε 6 800); ^{1}H NMR (DMSO-d_6) δ 0.85–0.93 (m, 2H, 2 x Hγ), 0.95–1.02 (m, 1H, CH cyclopropyl), 1.46–1.56 (m, 2H, 2 x Hβ), 1.99–2.14 (m, 2H, 2 x Hβ), 2.72–2.83 (m, 2H, 2 x Hα), 3.00–3.04 (m, 0.5H, Hα), 3.05–3.08 (m, 0.5H, Hα), 3.16–3.18 (d, *J* = 5.2 Hz, 1H, Hα), 3.50 (dd, *J* = 2.5, 12.0 Hz, 1H, H5′), 3.59–3.62 (m, 1H, H5′), 3.85–3.89 (m, 1H, H4′), 3.95–4.01 (m, 1H, H3′), 4.10 (“q”, *J* = 4.6 Hz, 1H, H2′), 4.36 (t, *J* = 4.9Hz, 1H, OH), 5.09–5.14 (m, 2H, 2 x OH), 5.51–5.55 (m, 1H, OH), 5.78 (d, *J* = 4.0 Hz, 0.5H, H1′), 5.79 (d, *J* = 3.9 Hz, 0.5H, H1′), 8.52 (s, 0.5H, H2), 8.53 (s, 0.5H, H2); HRMS (ESI$^+$) m/z calcd $C_{19}H_{27}N_5O_7$ $(M+H)^+$: 436.1827, found: 436.1829.

5-(1,2,3-Triazol-1*H*-yl)uridine-biotin adduct (24)—Cyclooctyne **6** (11.0 mg, 0.02 mmol) was added to a stirred solution of 5-azidouridine **21** (5.6 mg, 0.02 mmol) in a mixture of ACN/H_2O (3:1, 1 mL) at ambient temperature. After 3 min, the volatiles were evaporated *in vacuo* to give cycloadduct **24** (16.0 mg, 98%) as a white solid: HRMS (ESI$^+$) *m/z* calcd $C_{36}H_{53}N_9O_{12}S$ $(M+H)^+$: 836.3607, found: 836.3562.

2′-Deoxy-8-(1,2,3-triazol-1*H*-yl)uridine-OCT adduct (25)—Cyclooctyne **5** (4.7:1 *exo-endo* mixture; 14.3 mg, 0.1 mmol) was added to a stirred solution of $\mathbf{22}_{70}$ (26.7 mg, 0.1 mmol) in a mixture of ACN/H_2O/MeOH (3:1:1, 1 mL) at ambient temperature. After 15 min, the volatiles were evaporated *in vacuo* to give cycloadduct **25** as mixture of isomers (~1:1; 15.3 mg, 100%) as a white solid: ^{1}H NMR (DMSO-d_6) δ 0.83–0.94 (m, 2H, 2 x Hγ), 0.95–1.05 (m, 1H, CH cyclopropyl), 1.42–1.59 (m, 2H, 2 x Hβ), 1.98–2.14 (m, 2H, 2 x Hβ), 2.20 (“t”, *J* = 5.2 Hz, 2H, H2′ & H2′), 2.46–2.56 (m, 1H, Hα), 2.70–2.83 (m, 2H, 2 x Hα), 3.00–3.05 (m, 0.5H, Hα), 3.05–3.09 (m, 0.5H, Hα), 3.44–3.54 (m, 3H, H5′ & CH_2), 3.54–3.61 (m, 1H, H5″), 3.80 (q, *J* = 3.2 Hz, 1H, H4′), 4.17–4.26 (m, 1H, H3′), 4.34 (m, 1H, OH), 5.02 (m, 1H, OH), 5.28 (m, 1H, OH), 6.15 (t, *J* = 6.3 Hz, 0.5H, H1′), 6.16 (t, *J* = 6.3 Hz, 0.5H, H1′), 8.43 (s, 0.5H, H6), 8.44 (s, 0.5H, H6); HRMS (ESI$^+$) *m/z* calcd $C_{19}H_{26}N_5O_6$ $(M+H)^+$: 420.1878, found: 420.1878.

5-(1,2,3-Triazol-1*H*-yl)uridine-DBCO adduct (26)—Cyclooctyne **12** (5.6 mg, 0.02 mmol) was added to a stirred solution of **21** (5.5 mg, 0.02 mmol) in MeOH (1 mL) at ambient temperature. After 15 min, the volatiles were evaporated *in vacuo* and the residue was passed through a 0.2 μm PTFE syringe filter, and then injected into a semipreparative HPLC column (40% ACN/H_2O, 1.0 mL/min; t_R = 7.0–12.0 min) to give **26** as an inseparable mixture of isomers (5.1 mg, 77%): UV λ_{max} 276 nm (ε 7300), 291 nm (ε 7100), λ_{sh} 309 nm (ε 5400), λ_{min} 265 nm (ε 6750), 283 nm (ε 7000), 303 nm (ε 5000); HRMS (ESI$^+$) *m/z* calcd $C_{27}H_{28}N_9O_7$ $(M+H)^+$: 562.2045, found: 526.2040.

5-(1,2,3-Triazol-1*H*-yl)uridine-MFCO adduct (27)—Cyclooctyne **16** (7.6 mg, 0.02 mmol) was added to a stirred solution of 5-azidouridine **21** (5.6 mg, 0.02 mmol) in MeOH (1

mL) at ambient temperature. After 12 min, the volatiles were evaporated *in vacuo* to give complete conversion to cycloadduct **27** as mixture of regioisomers (1:1; 12.9 mg, 100%) as a white solid: UV λ_{max} 269 nm (ε 7100), λ_{min} 244 nm (ε 5000); ^{1}H NMR (DMSO-d_6) δ 1.40–1.50 (m, 6H, 3 x CH_2), 1.73–1.81 (m, 2H, CH_2), 2.27–2.34 (m, 2H, CH_2), 1.57–1.67 (m, 6H, 3 x CH_2), 2.48–2.53 (m, 2H, CH_2), 2.62–2.69 (m, 2H, CH_2), 2.78–2.86 (s, 4H, 2 x CH_2), 3.01–3.13 (m, 2H, CH_2), 3.47–3.54 (m, 1H, H5′), 3.60–3.65 (m, 1H, H5″), 3.94–3.99 (m, 1H, H4′), 4.08–4.15 (m, 1H, H3′), 4.27–4.36 (m, 1H, H2′), 5.06–5.11 (m, 2H, OH (2′) & OH (3′)), 5.51 (t, *J* = 6.7 Hz, 1H, OH (5′)), 5.78 (d, *J* = 4.9 Hz, 0.5 H, H1′), 5.79 (d, *J* = 4.6 Hz, 0.5 H, H1′), 8.57 (s, 1H, H6); HRMS (ESI$^+$) *m/z* calcd $C_{28}H_{36}FN_7O_{11}$ $(M+H)^+$: 666.2530, found: 666.2518.

8-(1,2,3-Triazol-1*H*-yl)adenosine-OCT adduct triphosphate (29)—Cyclooctyne **5** (5.6 mg, 0.01 mmol) was added to a stirred solution of 8-azidoadenosine 5′-triphosphate tetralithium salt **28** (3.2 mg, 0.01 mmol) in a mixture of ACN/H_2O (3:1, 1 mL) at ambient temperature. After 2 h, the volatiles were evaporated *in vacuo* to give **29** (3.2 mg, 92%) as a 1:1 mixture of regioisomers: ^{1}H NMR (ACN-d_3/D_2O) δ 0.80–0.88 (m, 2H, 2 x Hγ), 0.95–1.06 (m, 1H, CH cyclopropyl), 1.46–1.6 (m, 2H, 2 x Hβ), 2.06–2.28 (m, 2H, 2 x Hβ), 2.62–2.74 (m, 1H, Hα), 2.82–3.00 (m, 2H, 2 x Hα), 3.11–3.21 (m, 1H, Hα), 3.56–3.64 (m, 4H, H5′, H5′ & CH_2), 4.17–4.32 (m, 2H, H3′ & H4′), 4.89 (t, *J* = 5.8 Hz, 0.5H, H2′), 4.97 (t. *J* = 5.7 Hz, 0.5H, H2′), 5.47 (d, *J* = 5.6 Hz, 0.5H, H1′), 5.51 (d, *J* = 5.5 Hz, 0.5H, H1′), 8.32 (s, 0.5H, H2), 8.33 (s, 0.5H, H2); HRMS (ESI$^-$) *m/z* calcd $C_{20}H_{28}N_8O_{14}P_3$ $(M+H)^-$: 697.0943, found: 697.0962.

Photophysical Characterization

The fluorescent properties of the triazole products were determined using samples of varying concentration but whose absorbance at the excitation wavelength did not exceed 0.1 absorbance units. For determination of Φ_F the absorbance was kept below 0.06 and quinine sulfate in 100 mM sulfuric acid was used as reference standard (Φ_F = 0.55).[95] All samples were prepared in HPLC grade MeOH or DMSO and in freshly prepared 50 mM phosphate buffer, and placed in a 2 × 10 mm quartz cuvette at 18 °C. Absorption spectra were measured using a single beam UV–Vis spectrophotometer. Steady-state excitation and emission spectra were measured on a PC1 spectrofluorometer with bandwidth and slit width for excitation/emission set at 2 nm. Frequency-domain fluorescence lifetime measurements were performed using a ChronosFD spectrofluorometer. Samples were excited with a frequency modulated 280 nm LED and emission was collected using a 305 nm long pass filters (Andover); 2,5- Diphenyloxazole (PPO) solubilized in ethanol was used as a lifetime reference (τ =1.4 ns).[96] Modulation-phase data were fitted by a multiple-exponential decay model using GlobalsWE software and the residual and χ^2 parameter was used as criterion for goodness of fit.

MTT Assay

MCF-7 cells were seeded in 96-well plates at a density of 1 × 10^4 cells/mL and treated with different concentrations of azides **2** or **21** and cyclooctyne **5** for 24 h at 37 °C in a 5% CO^2 incubator. Methylthiazoletetrazolium (MTT) solution (5 mg/mL) was added to the assay mixture and incubated for 4 h. The culture media was removed prior to addition of DMSO.

The optical density of the solution was measured at 595 nm, using an absorbance microplate reader (Bio-Tek). Cells without the treatment of the compounds were used as the control. The cell viability percentage was calculated by the following formula: Cell viability percentage (%) = OD sample/OD control × 100%.

Cellular Permeability Measurements

Parallel artificial membrane permeability assay (PAMPA) was used to determine effective permeability coefficients P_e (centimeters per second), in a 96-well microtiter filter plates, on polycarbonate filter of 0.45 μm pore size, 10 μm thickness (Millipore AG, Volketswil, Switzerland), according to the procedure of Wohnsland and Faller.[82]

Each well was coated with 15 μL of lecitin (1% or 4% in dodecane solution) for 5 minutes avoiding pipette tip contact with the membrane. Compounds **2**, **4**, **11**, **19**, **20**, and **23** were dissolved in 5% DMSO in PBS solution (75 μM) and were tested at least in triplicate. The solution of each compound (300 μL each) was added to each well of the donor plate. Aqueous buffer (PBS) (300 μL) was added to each well of the acceptor plate and then the donor plate was placed upon the acceptor plate. The resulting chamber was incubated at ambient temperature for 16 h at ambient temperature under gentle shaking. After incubation, it was carefully disassembled and each well of the acceptor plate was analyzed using UV-Vis for compound concentration. A solution of each compound at its theoretical equilibrium (i.e., the resulting concentration of the donor and acceptor phases were simply combined) was similarly analyzed. The effective permeability (Log P_e) was calculated from the equation as reported.[82]

Cell Microscopy Studies

Fluorescent Microscopy. Typical Procedure—The MCF-7 cells (5×10^5 cells/mL) were seeded in an eight chambered coverglass system (1.5 German borosilicate coverglass, Lab-Tek II) and incubated at 37 °C overnight in Dulbecco's modified Eagle's medium (DMEM/F12 (1:1) 1X, 1.5 ml) containing 5% fetal bovine serum (FBS). The 8-azido-9-(β-D-arabinofuranosyl)adenine **2** in the reduced serum medium (1 μM) was added to the cells. After 4h, the cells were washed three times with fresh PBS (pH 7.5) media to remove any azide from the exterior portions of the cells. The cyclooctyne reagent **5** in reduced serum medium (1 μM) was then added to the medium and the cells were incubated at 37 °C for 16 h. The cells were then washed three times with fresh PBS (pH 7.5) media to remove any click adduct from the exterior portions of the cells and observed with a DV ELITE-microscope (Fisher Scientific) using excitation and absorbance filters were 360/40 and 470/40 nm, respectively.

In the first negative control, the MCF-7 cells were just incubated with azide **2** without the cyclooctyne reagent added. In the second negative control, the MCF-7 cells were just incubated with cyclooctyne **5**. Also, in the positive control the cells were treated with click adduct **11** dissolved in culture media. We used 0.1% trypan blue in the culture media before imaging the cells in DV ELITE microscope.

Note: In parallel experiments Lipofectamine LTX was used as liposome carrier.

Fluorescent Lifetime Imaging Microscopy (FLIM). Typical Procedure— Synthetically prepared triazole adduct **8**, **20** or **23** as well as *in vivo* generated **8** [0.5 mL of 1 μM solution in DMEM/F12 (1:1) 1X media] was added to MCF-7 cells (~50% cell confluency) cultured on slides mounted with 1-tissue culture well. After 24 h, the cells were washed twice with fresh (DMEM/F12 (1:1) 1X, 0.5 ml). The cells were then imaged at ambient temperature in fresh DMEM/F12 (~0.2 mL).

Ex vivo lifetime measurements were acquired using a custom-assembled frequency-domain upright FLIM system from Intelligent Imaging Innovations Inc. (3i). A continuous–wave excitation source (488 nm Argon laser) was modulated by a Pockels cell electro-optic modulator, which was synchronized with a Lambert Instruments II18MD gated image intensifier and CoolSnap EZ camera. A Yokogawa CSU-X1 spinning disk provided confocal scanning for fast image acquisition. A Zeiss W Plan-Apochromat 63x (n.a. 1.0) water-immersion objective lens and a Semrock 520 emission filters with a Semrock Di10 T488/568 diochroic were also used.

Image intensification was maintained at 2800 units across all experiments. Exposure times were set to acquire enough signal to span approximately 75% of the CCD's dynamic range, however this time was never extended to more than 40 seconds (as such samples typically have low signal-to-noise. System calibration was performed with the fluorescent dye, 1-hydroxypyrene-3,6,8-trisulfonate (HPTS), in solution (PBS at pH 7.5) for a standard lifetime of 5.4 ns. We found HPTS to be a reliable standard and superior to fluorescein, owing to its greater stability over time and pH shifts.

Supplementary Material

Refer to Web version on PubMed Central for supplementary material.

Acknowledgments

We thank NIH (1SC1CA138176, SFW; 1SC3GM084827, QF), NSF (MCB 1021831, JM), and NIMH (1F30MH097427, NS) for partial financial support. J.Z. is grateful to the MBRS RISE program (NIGMS; R25 GM61347) for her fellowship. N.S. is grateful to the Lois Pope Life Foundation for his fellowship. We thank Drs. Joong-ho Moon, Eladio Mendez and Deodutta Roy from FIU for their helpful discussions.

ABBREVIATIONS

DBCO	dibenzylcyclooctyne
FD-FLIM	frequency domain fluorescence lifetime imaging
MFCO	monofluorocyclooctyne
MTT	3-(4,5-dimethylthiazol-2-yl)-2,5-diphenyltetrazolium bromide
OCT	cyclopropyl cyclooctyne
ODNs	oligodeoxynucleotides
SPAAC	strain promoted click chemistry

References

1. Hein CD, Liu XM, Wang D. Click chemistry, a powerful tool for pharmaceutical sciences. Pharm Res. 2008; 25:2216–2230. [PubMed: 18509602]
2. Nwe K, Brechbiel MW. Growing applications of “click chemistry” for bioconjugation in contemporary biomedical research. Cancer Biother Radiopharm. 2009; 24:289–302. [PubMed: 19538051]
3. Yang PY, Wang M, He CY, Yao SQ. Proteomic profiling and potential cellular target identification of K11777, a clinical cysteine protease inhibitor, in Trypanosoma brucei. Chem Commun. 2012; 48:835–837.
4. Agard NJ, Prescher JA, Bertozzi CR. A Strain-Promoted [3 + 2] Azide–Alkyne Cycloaddition for Covalent Modification of Biomolecules in Living Systems. J Am Chem Soc. 2004; 126:15046–15047. [PubMed: 15547999]
5. Baskin JM, Prescher JA, Laughlin ST, Agard NJ, Chang PV, Miller IA, Lo A, Codelli JA, Bertozzi CR. Copper-free click chemistry for dynamic in vivo imaging. Proc Natl Acad Sci USA. 2007; 104:16793–16797. [PubMed: 17942682]
6. Codelli JA, Baskin JM, Agard NJ, Bertozzi CR. Second-Generation Difluorinated Cyclooctynes for Copper-Free Click Chemistry. J Am Chem Soc. 2008; 130:11486–11493. [PubMed: 18680289]
7. Laughlin ST, Bertozzi CR. In Vivo Imaging of Caenorhabditis elegans Glycans. ACS Chem Biol. 2009; 4:1068–1072. [PubMed: 19954190]
8. Gordon CG, Mackey JL, Jewett JC, Sletten EM, Houk KN, Bertozzi CR. Reactivity of Biarylazacyclooctynones in Copper-Free Click Chemistry. J Am Chem Soc. 2012; 134:9199–9208. [PubMed: 22553995]
9. Ning X, Guo J, Wolfert MA, Boons GJ. Visualizing Metabolically Labeled Glycoconjugates of Living Cells by Copper-Free and Fast Huisgen Cycloadditions. Angew Chem Int Ed. 2008; 47:2253–2255.
10. Dommerholt J, Schmidt S, Temming R, Hendriks LJ, Rutjes FP, van Hest JC, Lefeber DJ, Friedl P, van Delft FL. Readily accessible bicyclononynes for bioorthogonal labeling and three-dimensional imaging of living cells. Angew Chem Int Ed Engl. 2010; 49:9422–9425. [PubMed: 20857472]
11. Debets MF, van Berkel SS, Schoffelen S, Rutjes FPJT, van Hest JCM, van Delft FL. Aza-dibenzocyclooctynes for fast and efficient enzyme PEGylation via copper-free (3+2) cycloaddition. Chem Commun. 2010; 46:97–99.
12. Jawalekar AM, Malik S, Verkade JMM, Gibson B, Barta NS, Hodges JC, Rowan A, van Delft FL. Oligonucleotide Tagging for Copper-Free Click Conjugation. Molecules. 2013; 18:7346–7363. [PubMed: 23884112]
13. Laughlin ST, Baskin JM, Amacher SL, Bertozzi CR. In Vivo Imaging of Membrane-Associated Glycans in Developing Zebrafish. Science. 2008; 320:664–667. [PubMed: 18451302]
14. Belardi B, de la Zerda A, Spiciarich DR, Maund SL, Peehl DM, Bertozzi CR. Imaging the Glycosylation State of Cell Surface Glycoproteins by Two-Photon Fluorescence Lifetime Imaging Microscopy. Angew Chem Int Edit. 2013; 52:14045–14049.
15. Kore AR, Charles I. Click Chemistry Based Functionalizations of Nucleoside, Nucleotide and Nucleic Acids. Curr Org Chem. 2013; 17:2164–2191.
16. Sekhon BS. Click chemistry: current developments and applications in drug discovery. J Pharm Educ Res. 2012; 3:77–85.
17. El-Sagheer AH, Brown T. Click chemistry with DNA. Chem Soc Rev. 2010; 39:1388–1405. [PubMed: 20309492]
18. Xiong H, Leonard P, Seela F. Construction and Assembly of Branched Y-Shaped DNA: “Click” Chemistry Performed on Dendronized 8-Aza-7-deazaguanine Oligonucleotides. Bioconjugate Chem. 2012; 23:856–870.
19. Dyrager C, Borjesson K, Diner P, Elf A, Albinsson B, Wilhelmsson LM, Grotli M. Synthesis and Photophysical Characterisation of Fluorescent 8-(1H-1,2,3-Triazol-4-yl)adenosine Derivatives. Eur J Org Chem. 2009; 2009:1515–1521.

20. Pujari SS, Seela F. Parallel Stranded DNA Stabilized with Internal Sugar Cross- Links: Synthesis and Click Ligation of Oligonucleotides Containing 2′-Propargylated Isoguanosine. J Org Chem. 2013; 78:8545–8561. [PubMed: 23915305]
21. Berndl S, Herzig N, Kele P, Lachmann D, Li X, Wolfbeis OS, Wagenknecht HA. Comparison of a nucleosidic vs non-nucleosidic postsynthetic "click" modification of DNA with base-labile fluorescent probes. Bioconjugate Chem. 2009; 20:558–564.
22. Massi A, Nuzzi A, Dondoni A. Microwave-assisted organocatalytic anomerization of alpha-C-glycosylmethyl aldehydes and ketones. J Org Chem. 2007; 72:10279–10282. [PubMed: 18004870]
23. Isobe H, Fujino T, Yamazaki N, Guillot-Nieckowski M, Nakamura E. Triazole-linked analogue of deoxyribonucleic acid ((TL)DNA): design, synthesis, and double-strand formation with natural DNA. Org Lett. 2008; 10:3729–3732. [PubMed: 18656947]
24. Sirivolu VR, Vernekar SKV, Ilina T, Myshakina NS, Parniak MA, Wang Z. Clicking 3′-Azidothymidine into Novel Potent Inhibitors of Human Immunodeficiency Virus. J Med Chem. 2013; 56:8765–8780. [PubMed: 24102161]
25. Nuzzi A, Massi A, Dondoni A. Model Studies Toward the Synthesis of Thymidine Oligonucleotides with Triazole Internucleosidic Linkages Via Iterative Cu(I)-Promoted Azide–Alkyne Ligation Chemistry. QSAR & Comb Sci. 2007; 26:1191–1199.
26. Fujino T, Yamazaki N, Isobe H. Convergent synthesis of oligomers of triazolelinked DNA analogue (TLDNA) in solution phase. Tetrahedron Lett. 2009; 50:4101–4103.
27. Wu J, Yu W, Fu L, He W, Wang Y, Chai B, Song C, Chang J. Design, synthesis, and biological evaluation of new 2′-deoxy-2′-fluoro-4′-triazole cytidine nucleosides as potent antiviral agents. Eur J Med Chem. 2013; 63:739–745. [PubMed: 23570720]
28. Santner T, Hartl M, Bister K, Micura R. Efficient Access to 3′-Terminal Azide- Modified RNA for Inverse Click-Labeling Patterns. Bioconjugate Chem. 2014; 25:188–195.
29. Fomich MA, Kvach MV, Navakouski MJ, Weise C, Baranovsky AV, Korshun VA, Shmanai VV. Azide phosphoramidite in direct synthesis of azide-modified oligonucleotides. Org Lett. 2014; 16:4590–4593. [PubMed: 25156193]
30. Krause A, Hertl A, Muttach F, Jaschke A. Phosphine-Free Stille–Migita Chemistry for the Mild and Orthogonal Modification of DNA and RNA. Chem Eur J. 2014; 20:16613–16619. [PubMed: 25322724]
31. Fauster K, Hartl M, Santner T, Aigner M, Kreutz C, Bister K, Ennifar E, Micura R. 2′-Azido RNA, a versatile tool for chemical biology: synthesis, X-ray structure, siRNA applications, click labeling. ACS Chem Biol. 2012; 7:581–589. [PubMed: 22273279]
32. Aigner M, Hartl M, Fauster K, Steger J, Bister K, Micura R. Chemical Synthesis of Site-Specifically 2′-Azido-Modified RNA and Potential Applications for Bioconjugation and RNA Interference. ChemBioChem. 2011; 12:47–51. [PubMed: 21171007]
33. Beyer C, Wagenknecht HA. In situ azide formation and "click" reaction of nile red with DNA as an alternative postsynthetic route. Chem Commun. 2010; 46:2230–2231.
34. Wada T, Mochizuki A, Higashiya S, Tsuruoka H, Kawahara S-i, Ishikawa M, Sekine M. Synthesis and properties of 2-azidodeoxyadenosine and its incorporation into oligodeoxynucleotides. Tetrahedron Lett. 2001; 42:9215–9219.
35. Padilla R, Sousa R. A Y639F/H784A T7 RNA polymerase double mutant displays superior properties for synthesizing RNAs with non-canonical NTPs. Nucleic Acids Res. 2002; 30:e138. [PubMed: 12490729]
36. Weisbrod SH, Marx A. A nucleoside triphosphate for site-specific labelling of DNA by the Staudinger ligation. Chem Commun. 2007:1828–1830.
37. Weisbrod SH, Baccaro A, Marx A. DNA Conjugation by Staudinger Ligation. Nucleic Acids Symp Ser. 2008; 52:383–384.
38. Jawalekar AM, Meeuwenoord N, Cremers JS, Overkleeft HS, van der Marel GA, Rutjes FP, van Delft FL. Conjugation of nucleosides and oligonucleotides by [3+2] cycloaddition. J Org Chem. 2008; 73:287–290. [PubMed: 18052191]
39. Jayaprakash KN, Peng CG, Butler D, Varghese JP, Maier MA, Rajeev KG, Manoharan M. Non-nucleoside building blocks for copper-assisted and copper-free click chemistry for the efficient synthesis of RNA conjugates. Org Lett. 2010; 12:5410–5413. [PubMed: 21049912]

40. Suchy M, Milne M, Li AX, McVicar N, Dodd DW, Bartha R, Hudson RHE. Mono- and Tetraalkyne Modified Ligands and Their Eu3+ Complexes - Utilizing “Click” Chemistry to Expand the Scope of Conjugation Chemistry. Eur J Org Chem. 2011:6532–6543.

41. Gunji H, Vasella A. Oligonucleosides with a nucleobase-including backbone- part 4: a convergent synthesis of ethynediyl-linked adenosine tetramers. Helv Chim Acta. 2000; 83:3229–3245.

42. Cosyn L, Palaniappan KK, Kim SK, Duong HT, Gao ZG, Jacobson KA, Van Calenbergh S. 2-Triazole-substituted adenosines: A new class of selective A(3) adenosine receptor agonists, partial agonists, and antagonists. J Med Chem. 2006; 49:7373–7383. [PubMed: 17149867]

43. Gupte A, Boshoff HI, Wilson DJ, Neres J, Labello NP, Somu RV, Xing CG, Barry CE, Aldrich CC. Inhibition of Siderophore Biosynthesis by 2-Triazole Substituted Analogues of 5′-O-[N-(Salicyl)sulfamoyl]adenosine: Antibacterial Nucleosides Effective against Mycobacterium tuberculosis. J Med Chem. 2008; 51:7495–7507. [PubMed: 19053762]

44. Lakshman MK, Kumar A, Balachandran R, Day BW, Andrei G, Snoeck R, Balzarini J. Synthesis and Biological Properties of C-2 Triazolylinosine Derivatives. J Org Chem. 2012; 77:5870–5883. [PubMed: 22758929]

45. Hong V, Steinmetz NF, Manchester M, Finn MG. Labeling Live Cells by Copper-Catalyzed Alkyne–Azide Click Chemistry. Bioconjugate Chem. 2010; 21:1912–1916.

46. When this work was in progress Ito et al. reported an example of the SPAAC between the 8- azido-cAMP and a difluorinated cyclooctyne in HeLa cells see: Ito K, Liu H, Komiyama M, Hayashi T, Xu Y. Direct Light-up of cAMP Derivatives in Living Cells by Click Reactions. Molecules. 2013; 18:12909–12915. [PubMed: 24141242]

47. Zhang, B.; Wang, W.; Qu, D. Patent Appl. CN101550175A. 2009.

48. Gourdain S, Martinez A, Petermann C, Harakat D, Clivio P. Unraveling the photochemistry of the 5-azido-2′-deoxyuridine photoaffinity label. J Org Chem. 2009; 74:6885–6887. [PubMed: 19653622]

49. Neef AB, Luedtke NW. An azide-modified nucleoside for metabolic labeling of DNA. ChemBioChem. 2014; 15:789–793. [PubMed: 24644275]

50. Marks IS, Kang JS, Jones BT, Landmark KJ, Cleland AJ, Taton TA. Strain-Promoted “Click” Chemistry for Terminal Labeling of DNA. Bioconjugate Chem. 2011; 22:1259–1263.

51. Shelbourne M, Chen X, Brown T, El-Sagheer AH. Fast copper-free click DNA ligation by the ring-strain promoted alkyne-azide cycloaddition reaction. Chem Commun. 2011; 47:6257–6259.

52. Singh I, Freeman C, Heaney F. Efficient Synthesis of DNA Conjugates by Strain- Promoted Azide-Cyclooctyne Cycloaddition in the Solid Phase. Eur J Org Chem. 2011; 2011:6739–6746.

53. Singh I, Freeman C, Madder A, Vyle JS, Heaney F. Fast RNA conjugations on solid phase by strain-promoted cycloadditions. Org Biomol Chem. 2012; 10:6633–6639. [PubMed: 22751955]

54. Other approaches including the click reaction between norbornenes and nitrile oxides for the modification of oligonucleotides have also been developed see: Gutsmiedl K, Wirges CT, Ehmke V, Carell T. Copper-Free “Click” Modification of DNA via Nitrile Oxide–Norbornene 1,3- Dipolar Cycloaddition. Org Lett. 2009; 11:2405–2408. [PubMed: 19405510]

55. Zimmet J, Jarlebark L, Hammarberg T, Van Galen PJM, Jacobson KA, Heilbronn E. Synthesis and Biological Activity of Novel 2-Thio Derivatives of ATP. Nucleosides Nucleotides. 1993; 12:1–20. [PubMed: 25181577]

56. Sinkeldam RW, Greco NJ, Tor Y. Fluorescent Analogs of Biomolecular Building Blocks: Design, Properties, and Applications. Chem Rev. 2010; 110:2579–2619. [PubMed: 20205430]

57. Ranasinghe RT, Brown T. Fluorescence based strategies for genetic analysis. Chem Commun. 2005:5487–5502.

58. Tanpure AA, Pawar MG, Srivatsan SG. Fluorescent Nucleoside Analogs: Probes for Investigating Nucleic Acid Structure and Function. Isr J Chem. 2013; 53:366–378.

59. Holmes RE, Robins RK. Purine nucleosides. IX The synthesis of 9-β-D-ribofuranosyluric acid and other related 8-substituted purine ribonucleosides. J Am Chem Soc. 1965; 87:1772–1776. [PubMed: 14289333]
60. Stewart JA, Wilson CJ, Swarts BM. Effect of Azide Position on the Rate of Azido Glucose–Cyclooctyne Cycloaddition. J Carbohydr Chem. 2014; 33:408–419.
61. Chattopadhyaya JB, Reese CB. Reaction between 8-Bromoadenosine and Amines - Chemistry of 8-Hydrazinoadenosine. Synthesis. 1977:725–726.
62. Buenger GS, Nair V. Dideoxygenated purine nucleosides substituted at the 8- position: chemical synthesis and stability. Synthesis. 1990:962–966.
63. Kuzmin A, Poloukhtine A, Wolfert MA, Popik VV. Surface Functionalization Using Catalyst-Free Azide-Alkyne Cycloaddition. Bioconjugate Chem. 2010; 21:2076–2085.
64. Schultz MK, Parameswarappa SG, Pigge FC. Synthesis of a DOTA--biotin conjugate for radionuclide chelation via Cu-free click chemistry. Org Lett. 2010; 12:2398–2401. [PubMed: 20423109]
65. Tworowska, I.; Sims-Mourtada, J.; Delpassand, ES. WO. 2012/177701 A2. 2012.
66. Chenoweth K, Chenoweth D, Goddard WA. Cyclooctyne-based reagents for uncatalyzed click chemistry: A computational survey. Org Biomol Chem. 2009; 7:5255–5258. [PubMed: 20024122]
67. Saenger, W. Principles of Nucleic Acid Structure. Springer; New York: 1984.
68. Ikehara M, Uesugi S, Yoshida K. Nucleosides and nucleotides. XLVII Conformation of purine mucleosides and their 5′-phosphates. Biochemistry. 1972; 11:830–836. [PubMed: 5059890]
69. Sarma RH, Lee CH, Evans FE, Yathindra N, Sundaralingam M. Probing the interrelation between the glycosyl torsion, sugar pucker, and the backbone conformation in C(8) substituted adenine nucleotides by proton and proton-phosphorus-31 fast Fourier transfer nuclear magnetic resonance methods and conformational energy calculations. J Am Chem Soc. 1974; 96:7337–7348. [PubMed: 4427056]
70. Gourdain S, Petermann C, Harakat D, Clivio P. Highly efficient and facile synthesis of 5-azido-2′-deoxyuridine. Nucleosides, Nucleotides Nucleic Acids. 2010; 29:542–546. [PubMed: 20589573]
71. Rayala R, Wnuk SF. Bromination at C-5 of pyrimidine and C-8 of purine nucleosides with 1,3-dibromo-5,5-dimethylhydantoin. Tetrahedron Lett. 2012; 53:3333–3336. [PubMed: 22773864]
72. Sletten EM, Bertozzi CR. A hydrophilic azacyclooctyne for Cu-free click chemistry. Org Lett. 2008; 10:3097–3099. [PubMed: 18549231]
73. Sun KM, McLaughlin CK, Lantero DR, Manderville RA. Biomarkers for phenol carcinogen exposure act as pH-sensing fluorescent probes. J Am Chem Soc. 2007; 129:1894–1895. [PubMed: 17256942]
74. Andreasson J, Holmen A, Albinsson B. The Photophysical Properties of the Adenine Chromophore. J Phys Chem B. 1999; 103:9782–9789.
75. Daniels M, Hauswirth W. Fluorescence of the Purine and Pyrimidine Bases of the Nucleic Acids in Neutral Aqueous Solution at 300°K. Science. 1971; 171:675–677. [PubMed: 5540307]
76. Nir E, Kleinermanns K, Grace L, de Vries MS. On the Photochemistry of Purine Nucleobases. J Phys Chem A. 2001; 105:5106–5110.
77. Noe MS, Rios AC, Tor Y. Design, Synthesis, and Spectroscopic Properties of Extended and Fused Pyrrolo-dC and Pyrrolo-C Analogs. Org Lett. 2012; 14:3150–3153. [PubMed: 22646728]
78. O'Mahony G, Ehrman E, Grotli M. Synthesis and photophysical properties of novel cyclonucleosides—substituent effects on fluorescence emission. Tetrahedron. 2008; 64:7151–7158.
79. Manderville RA, Omumi A, Rankin KM, Wilson KA, Millen AL, Wetmore SD. Fluorescent C-Linked C-8-Aryl-guanine Probe for Distinguishing syn from anti Structures in Duplex DNA. Chem Res Toxicol. 2012; 25:1271–1280. [PubMed: 22667322]
80. Rankin KM, Sproviero M, Rankin K, Sharma P, Wetmore SD, Manderville RA. C8-Heteroaryl-2′-deoxyguanosine Adducts as Conformational Fluorescent Probes in the NarI Recognition Sequence. J Org Chem. 2012; 77:10498–10508. [PubMed: 23171213]
81. Striker G, Subramaniam V, Seidel CAM, Volkmer A. Photochromicity and fluorescence lifetimes of green fluorescent protein. J Phys Chem B. 1999; 103:8612–8617.

82. Wohnsland F, Faller B. High-Throughput Permeability pH Profile and High- Throughput Alkane/Water log P with Artificial Membranes. J Med Chem. 2001; 44:923–930. [PubMed: 11300874]
83. Kansy M, Senner F, Gubernator K. Physicochemical High Throughput Screening: Parallel Artificial Membrane Permeation Assay in the Description of Passive Absorption Processes. J Med Chem. 1998; 41:1007–1010. [PubMed: 9544199]
84. Sugano K, Nabuchi Y, Machida M, Aso Y. Prediction of human intestinal permeability using artificial membrane permeability. Int J Pharm. 2003; 257:245–251. [PubMed: 12711179]
85. Fujikawa M, Nakao K, Shimizu R, Akamatsu M. QSAR study on permeability of hydrophobic compounds with artificial membranes. Biorg Med Chem. 2007; 15:3756–3767.
86. Fujikawa M, Ano R, Nakao K, Shimizu R, Akamatsu M. Relationships between structure and high-throughput screening permeability of diverse drugs with artificial membranes: Application to prediction of Caco-2 cell permeability. Biorg Med Chem. 2005; 13:4721–4732.
87. Molina-Arcas M, Casado FJ, Pastor-Anglada M. Nucleoside transporter proteins. Curr Vasc Pharmacol. 2009; 7:426–434. [PubMed: 19485885]
88. Lee J, Twomey M, Machado C, Gomez G, Doshi M, Gesquiere AJ, Moon JH. Caveolae-Mediated Endocytosis of Conjugated Polymer Nanoparticles. Macromol Biosci. 2013; 13:913–920. [PubMed: 23629923]
89. Berezin MY, Achilefu S. Fluorescence Lifetime Measurements and Biological Imaging. Chem Rev. 2010; 110:2641–2684. [PubMed: 20356094]
90. Seksek O, Bolard J. Nuclear pH gradient in mammalian cells revealed by laser microspectrofluorimetry. J Cell Sci. 1996; 109:257–262. [PubMed: 8834810]
91. Yoo H, Yang J, Yousef A, Wasielewski MR, Kim D. Excimer formation dynamics of intramolecular pi-stacked perylenediimides probed by single-molecule fluorescence spectroscopy. J Am Chem Soc. 2010; 132:3939–3944. [PubMed: 20184367]
92. Islam MS, Honma M, Nakabayashi T, Kinjo M, Ohta N. pH Dependence of the Fluorescence Lifetime of FAD in Solution and in Cells. Int J Mol Sci. 2013; 14:1952–1963. [PubMed: 23334475]
93. Haga Y, Ishii K, Hibino K, Sako Y, Ito Y, Taniguchi N, Suzuki T. Visualizing specific protein glycoforms by transmembrane fluorescence resonance energy transfer. Nat Commun. 2012; 3:907–913. [PubMed: 22713749]
94. Schaeffer HJ, Thomas HJ. Synthesis of potential anticancer agents. XIV Ribosides of 2,6-disubstituted purines. J Am Chem Soc. 1958; 80:3738–3742.
95. Eaton DF. Reference Materials for Fluorescence Measurement. Pure Appl Chem. 1988; 60:1107–1114.
96. Lukavenko ON, Eltsov SV, Grigorovich AV, McHedlov-Petrossyan NO. Solubility and fluorescence lifetime of 2,5-diphenyloxazole and 1,4-bis(5-phenyl-oxazolyl-2)benzene in water–ethanol and water–acetone solvent systems. J Mol Liq. 2009; 145:167–172.

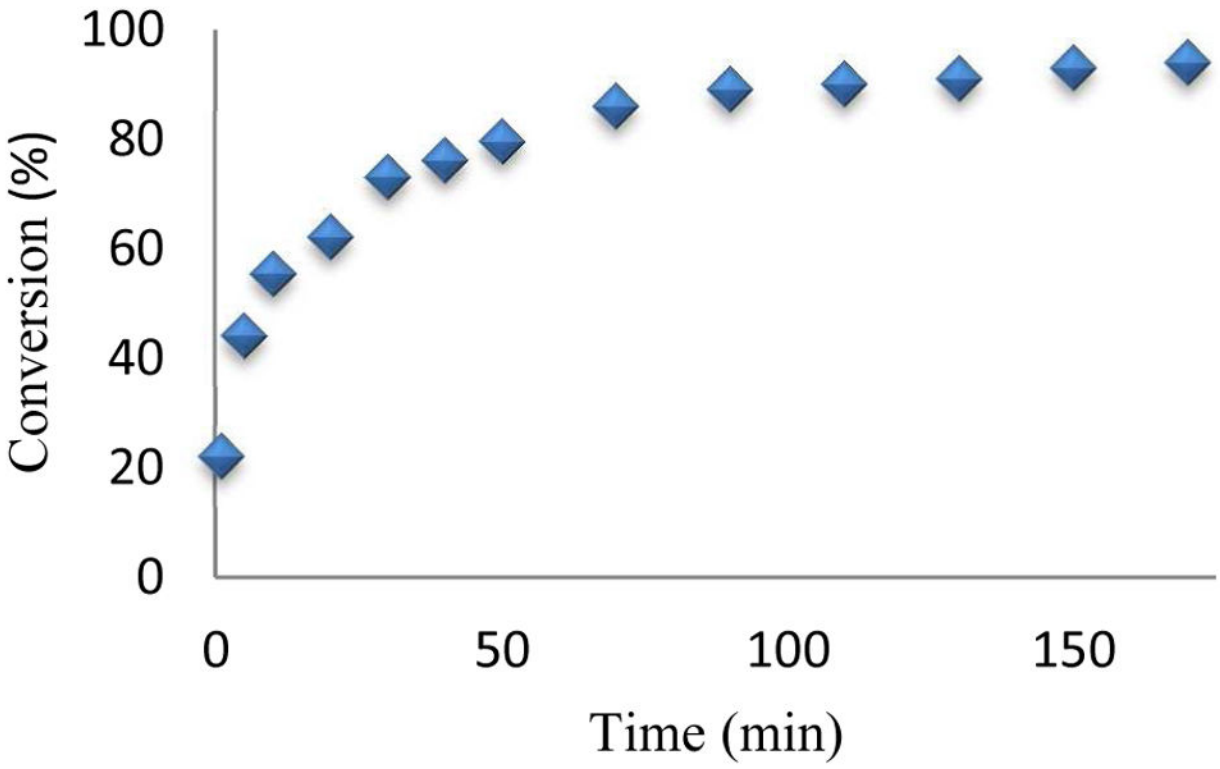

Figure 1.

The kinetic profile of the SPAAC reaction of the equivalent amount of 8-azidoadenosine **1** and cyclooctyne **5** in ACN-d_6/D_2O (3:1, *v/v*; 23 mM) as monitored by ^1H NMR.

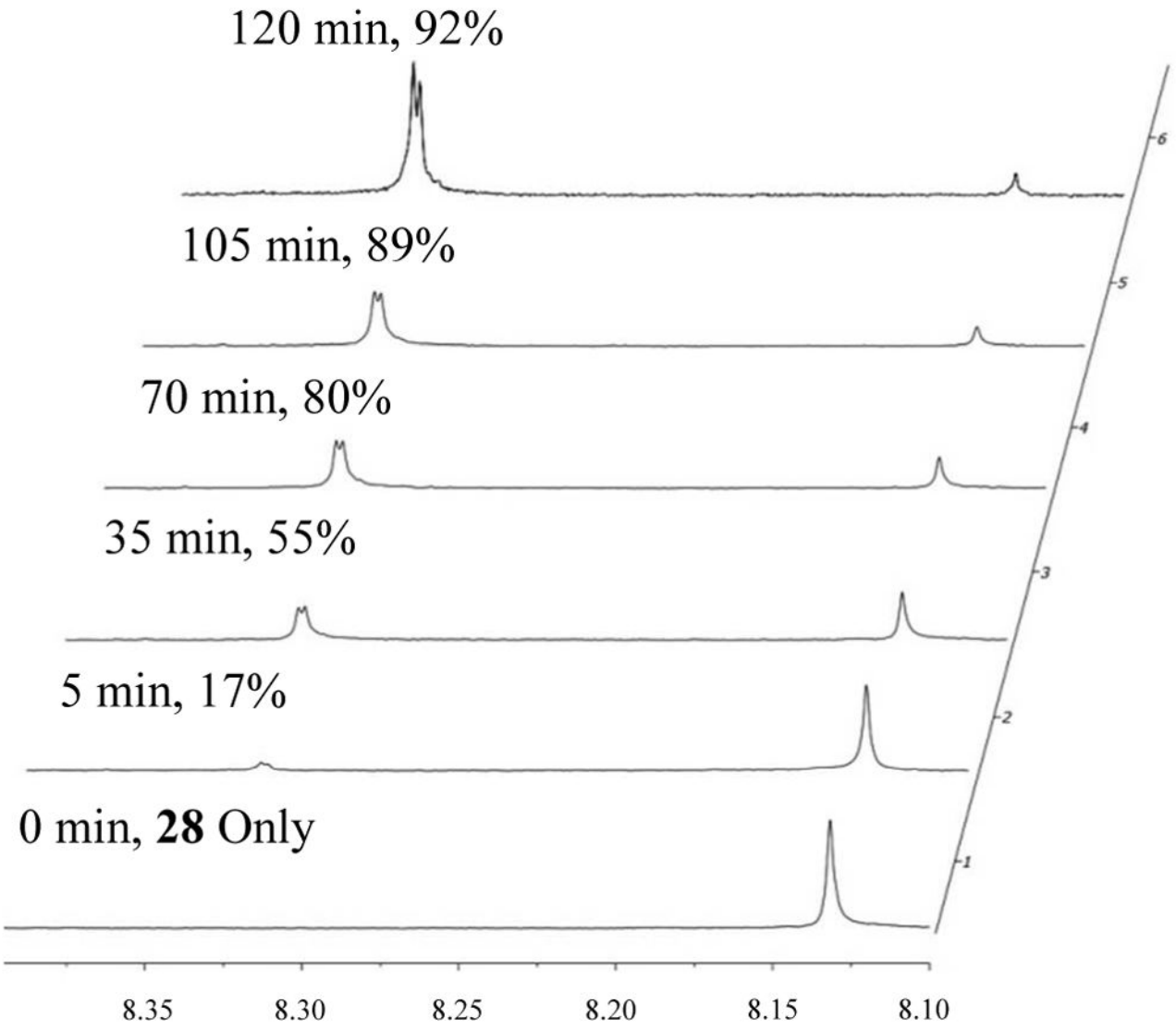

Figure 2.

The kinetic profile of the reaction between azidonucleotide **28** and cyclooctyne **5** in ACN-d_6/D_2O (3:1, *v/v*; 6 mM) as monitored by ^1H NMR.

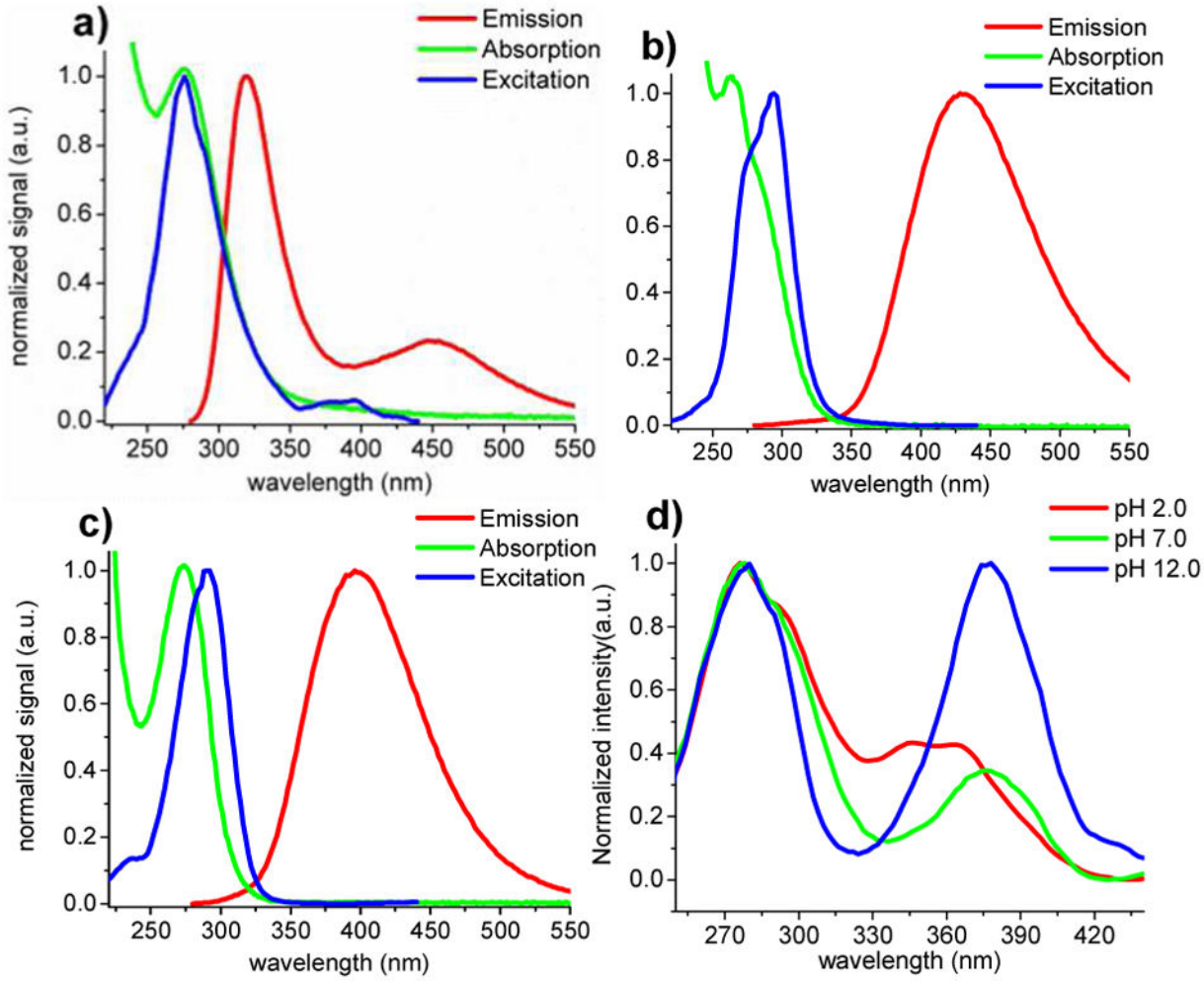

Figure 3.

Normalized fluorescence emission, absorption and excitation spectra for the selected click adducts: a) **23**, b) **11**, and c) **20** in MeOH; (d) The pH effect on the excitation spectra of **23** in phosphate buffer.

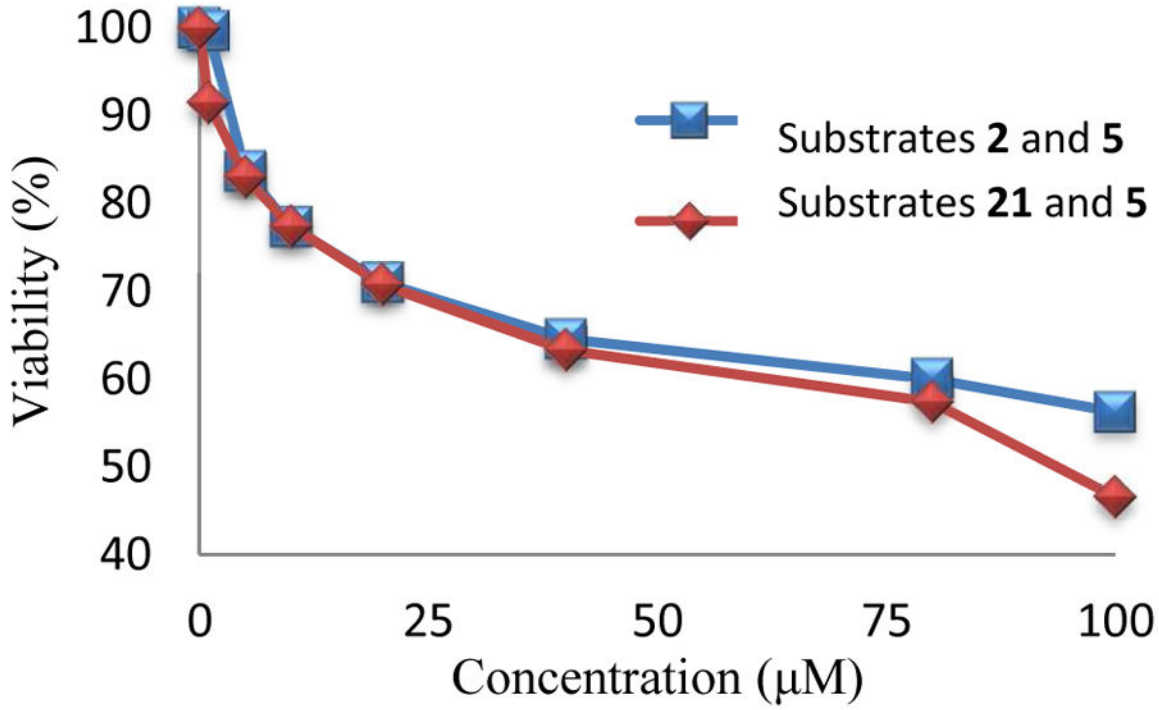

Figure 4.
Cellular viability of MCF-7 cells when exposed to the click reactions between azides **2** or **21** and cyclooctyne **5**.

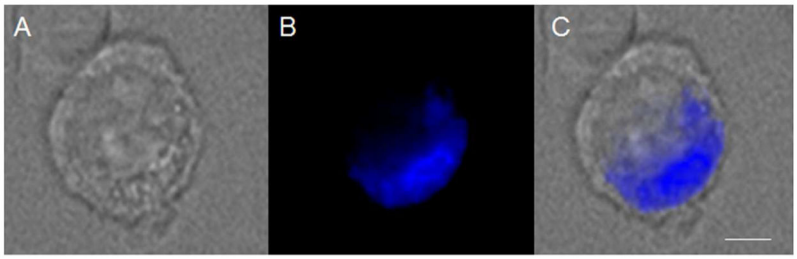

Figure 5.

Fluorescence microscopy images and phase photos of live cells: (A) Phase photo of MCF-7 cells after the reaction of azide **2** with cyclooctyne **5**; (B) Fluorescent photo of the same MCF-7 cell; (C) Merged photo of panels (A) and (B). Scale = 20 μm

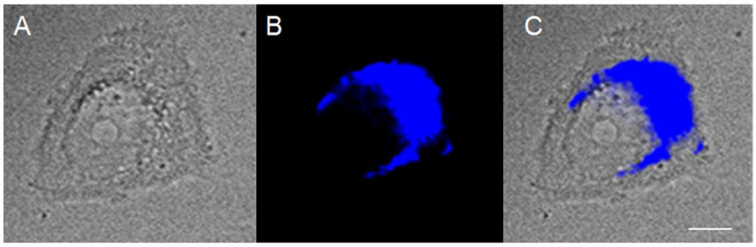

Figure 6.

Fluorescence microscopy images and phase photos of live cells: (A) Phase photo of MCF-7 cells after the reaction of azide **19** with cyclooctyne **12**; (B) Fluorescent photo of the same MCF-7 cell; (C) Merged photo of panels (A) and (B). Scale = 20 μm

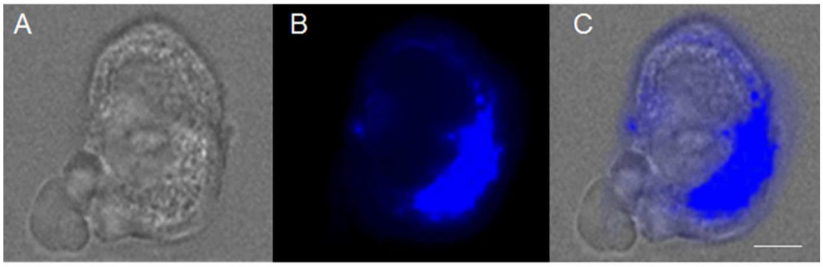

Figure 7.

Fluorescence microscopy images and phase photos of live cells: (A) Phase photo of MCF-7 cells after the reaction azide **21** with cyclooctyne **5**; (B) Fluorescent photo of the same MCF-7 cell; (C) Merged photo of panels (A) and (B). Scale = 20 μm

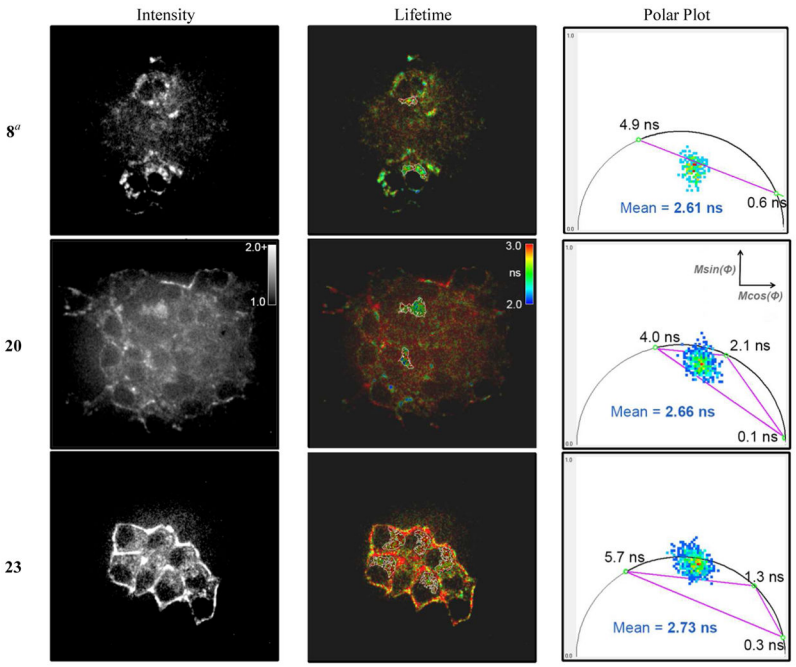

Figure 8.

Representative images of fluorescence intensity (left column), fluorescence lifetime (middle column), and Polar Plot histogram (right column) for triazole adducts **8**, **20** and **23** (1 μM) within MCF-7 cells. Fluorescence intensity images display an intensity range from 1.0 (background intensity) to 2.0+ (2x background and greater). Fluorescence lifetime heat maps display lifetimes ranging from 2.0 ns (and below) in blue to 3.0 ns (and above) in red. Polar plot histograms depict the x,y coordinates [Mcos(Φ_F), Msin(Φ_F)] of pixels within nuclei (outlined in the corresponding lifetime image). Experimental component lifetimes are indicated on the semi-circle (green circles), as well as the group mean lifetime for the specific compound. [a]Images for **8** are for the triazole adduct synthesized using an *in vivo* click reaction.

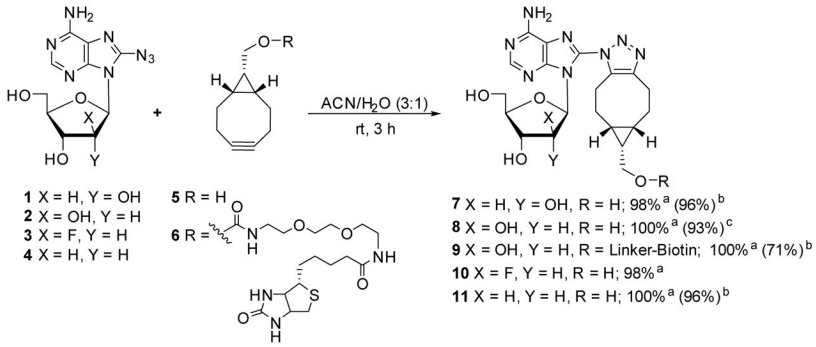

[a] Based on ^{1}H NMR, [b] Purified by RP HPLC, [c] Purified on silica gel column.

Scheme 1.

Strain Promoted Click Chemistry of 8-Azidoadenine Nucleosides

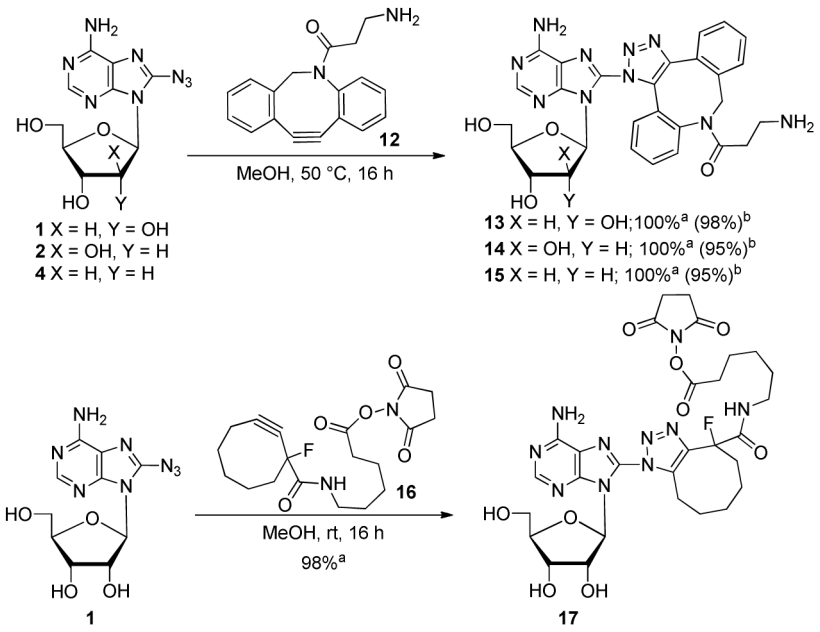

Scheme 2.

Strain Promoted Click Chemistry of 8-Azidoadenine Nucleosides with Dibenzyl or Monofluoro Cyclooctyne

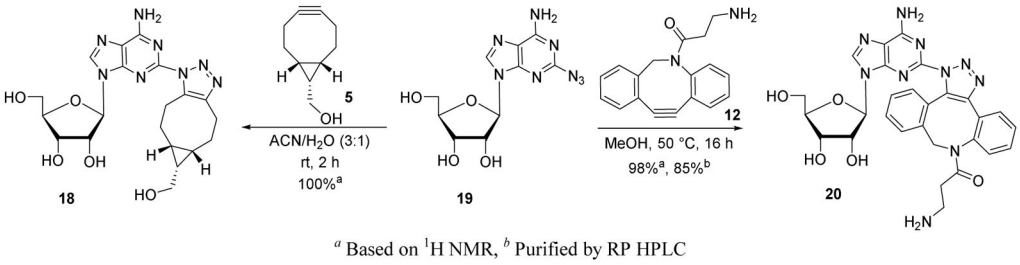

[a] Based on ^{1}H NMR, [b] Purified by RP HPLC

Scheme 3.
Strain Promoted Click Chemistry of 2-Azidoadenosine

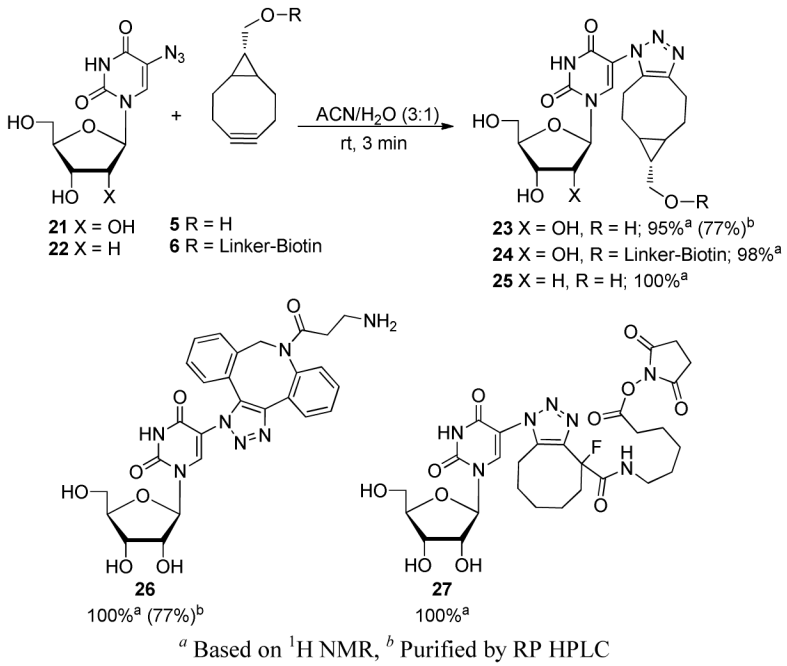

Scheme 4.

Strain Promoted Click Chemistry of 5-Azidouridine and 5-Azido-2′-deoxyuridine

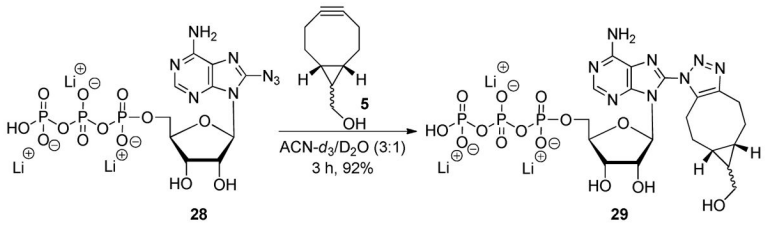

Scheme 5.

Strain Promoted Click Chemistry of 8-Azidoadenosine 5′-triphosphate 28

Table 1

Photophysical data for the selected triazole adducts.

	7	8	11	13	17	18	20	23	26	27
$\varepsilon_{max}(M^{-1}cm^{1})$	21100	17500	18200	16000	16400	19100	16400	10100	7300	7100
$\lambda_{max}(abs)^{a}(nm)$	270	273	272	276	271	261	263	270	276	269
$\lambda_{max}(exc)^{a}(nm)$	280	278	290	293	288	270	295	276	312	-
$\lambda_{max}(exc)^{a,d}(nm)$	309	-	-	360	-	329	-	388	370	-
$\lambda_{max}(emi)^{a}(nm)$	392	390	397	440	399	395	428	312	361	327/412
$\lambda_{max}(emi)^{b}(nm)$	376	384	392	429	397	375	422	324/440	-	331/419
$\lambda_{max}(emi)^{c}(nm)$	403	400	402	452	399	405	439	334/445	-	339/434
Stokes shift$^{a}(nm)$	83	112	107	80	111	66	133	44/62	49	58
$\Phi_{F}{}^{a}$	0.006	0.006	0.014	0.017	0.006	0.02	0.106	0.011	0.013	0.009
Brightness^{a} $(M^{-1}cm^{1})$	0.13	0.11	0.25	0.27	0.10	0.38	1.74	0.12	0.09	0.06
$\tau_{1}{}^{a}(ns)$	0.10	0.60	0.10	-	0.10	0.30	0.10	0.30	0.30	-
$\tau_{2}{}^{a}(ns)$	0.80	4.90	0.90	-	0.90	1.0	2.0	1.30	2.30	-
$\tau_{3}{}^{a}(ns)$	5.90	-	5.60	-	5.30	5.80	4.10	5.70	7.80	-
$\tau_{average}(ns)$	0.70	1.60	1.60	-	1.20	0.80	2.80	2.70	2.70	-
$f_{1}{}^{a}(\%)$	0.63	0.77	0.28	-	0.46	0.64	0.02	0.22	0.11	-
$f_{2}{}^{a}(\%)$	0.30	0.23	0.53	-	0.39	0.30	0.58	0.39	0.78	-
$f_{3}{}^{a}(\%)$	0.07	-	0.19	-	0.15	0.05	0.4	0.38	0.11	-

[a] In MeOH.

[b] In DMSO.

[c] In 50 mM phosphate buffer pH 7.0.

[d] Second maxima observed at the red edge of the excitation spectra.

Table 2

Cellular permeability data for the selected azides and triazole adduct.

Compound	% Fraction Absorbed	Log P_e (cm/s)[a]
2[b]	18	−0.5
4	20	−0.5
11	21	−0.3
19	22	−0.5
20	22	−0.03
23	20	−0.4

[a] Log of the effective permeability coefficient, P^e ($cm \cdot s^{-1}$), as assessed by a parallel artificial membrane permeability assay (HDM-PAMPA) performed at 75 μM concentrations.

[b] Permeability for **2** at a 150 μM concentration was also 18%.

Table 3

Mean lifetime of nucleoside triazole adducts within MCF-7 cells as determined by Frequency-Domain Lifetime Imaging (FD-FLIM).

Compound	Mean lifetime (ns)	SD	n (# nuclei)	SEM
8	2.66	0.159	13	0.044
8[a]	2.61	0.103	11	0.031
20	2.66	0.102	16	0.026
23	2.73	0.093	14	0.025

[a]Triazole adduct **8** synthesized by *in vivo* click reaction